

~~AD 300 870~~
DTIC FILE COPY AD

(12)

AD-A179 735

TECHNICAL REPORT BRL-TR-2781

HEMISPHERICAL AND CONICAL
SHAPED-CHARGE LINER COLLAPSE
AND JET FORMATION

WILLIAM P. WALTERS
STANLEY K. GOLASKI

FEBRUARY 1987

DTIC
ELECTE
APR 30 1987
S D

APPROVED FOR PUBLIC RELEASE; DISTRIBUTION UNLIMITED.

US ARMY BALLISTIC RESEARCH LABORATORY
ABERDEEN PROVING GROUND, MARYLAND

*Original contains color
plates; All DTIC reproduct-
ions will be in black and
white*

87 4 29 051

Destroy this report when it is no longer needed.
Do not return it to the originator.

Additional copies of this report may be obtained
from the National Technical Information Service,
U. S. Department of Commerce, Springfield, Virginia
22161.

The findings in this report are not to be construed as an official
Department of the Army position, unless so designated by other
authorized documents.

The use of trade names or manufacturers' names in this report
does not constitute indorsement of any commercial product.

Unclassified

SECURITY CLASSIFICATION OF THIS PAGE

AD-A179735

REPORT DOCUMENTATION PAGE

Form Approved
OMB No. 0704-0188
Exp. Date: Jun 30, 1986

1a. REPORT SECURITY CLASSIFICATION UNCLASSIFIED			1b. RESTRICTIVE MARKINGS		
2a. SECURITY CLASSIFICATION AUTHORITY			3. DISTRIBUTION / AVAILABILITY OF REPORT		
2b. DECLASSIFICATION / DOWNGRADING SCHEDULE					
4. PERFORMING ORGANIZATION REPORT NUMBER(S) BRL-TR-2781			5. MONITORING ORGANIZATION REPORT NUMBER(S)		
6a. NAME OF PERFORMING ORGANIZATION Ballistic Research Laboratory		6b. OFFICE SYMBOL (If applicable) SLCBR-TB	7a. NAME OF MONITORING ORGANIZATION		
6c. ADDRESS (City, State, and ZIP Code) Aberdeen Proving Ground, MD 21005-5066			7b. ADDRESS (City, State, and ZIP Code)		
8a. NAME OF FUNDING / SPONSORING ORGANIZATION		8b. OFFICE SYMBOL (If applicable)	9. PROCUREMENT INSTRUMENT IDENTIFICATION NUMBER		
8c. ADDRESS (City, State, and ZIP Code)			10. SOURCE OF FUNDING NUMBERS		
			PROGRAM ELEMENT NO.	PROJECT NO.	TASK NO.
11. TITLE (Include Security Classification) HEMISPHERICAL AND CONICAL SHAPED-CHARGE LINER COLLAPSE AND JET FORMATION					
12. PERSONAL AUTHOR(S) Walters, William P., Golaski, Stanley K.					
13a. TYPE OF REPORT Technical Report		13b. TIME COVERED FROM _____ TO _____		14. DATE OF REPORT (Year, Month, Day)	
15. PAGE COUNT					
16. SUPPLEMENTARY NOTATION COLOR REPORT (10 COLOR FIGURES)					
17. COSATI CODES			18. SUBJECT TERMS (Continue on reverse if necessary and identify by block number) Shaped-Charge, Jet Formation, Stratified, Bimetallic Liners, Hemispherical Liners, Jet Collapse, Diffusion Bonding, Conical Liners, Tubular Jet Formation		
FIELD	GROUP	SUB-GROUP			
19	01				
19. ABSTRACT (Continue on reverse if necessary and identify by block number) Analytical studies of the collapse of (1) hemispherical, point initiated, (2) hemispherical, surface initiated and (3) conical, point initiated warheads, using the HELP and EPIC hydrocodes predicted tubular or layered jets. Each shaped-charge geometry studied revealed a different flow pattern during the jet formation and collapse process. The analysis further suggested that the liner flow process could be verified experimentally by collapsing stratified, bimetallic liners in actual warheads.					
<p>Experimental verification was attempted by fabricating stratified bimetallic copper and nickel hemispherical and conical liners. Copper and nickel were chosen for the stratified liner materials due to their identical densities and similarity under shock loading conditions. The fabrication was successfully accomplished by using a diffusion bonding technique which with the appropriate temperature, time and pressure caused the alternating copper and nickel discs to adhere. The liners were then machined from this bonded stack of alternating layers of copper and nickel.</p>					
20. DISTRIBUTION / AVAILABILITY OF ABSTRACT <input type="checkbox"/> UNCLASSIFIED/UNLIMITED <input checked="" type="checkbox"/> SAME AS RPT. <input type="checkbox"/> DTIC USERS			21. ABSTRACT SECURITY CLASSIFICATION UNCLASSIFIED		
22a. NAME OF RESPONSIBLE INDIVIDUAL William P. Walters			22b. TELEPHONE (Include Area Code) 301/278-6062		22c. OFFICE SYMBOL SLCBR-TB-W

19. ABSTRACT (Cont'd)

Point initiated, Octol loaded, hemispherical and conical shaped charge warheads were then fired into water and typically, three to four large particles were recovered per shot. Examination of the recovered particles revealed agreement with the method of formation predicted by the two hydrocodes. Namely, the recovered particles showed the presence of two materials in alternating layers. Also, free flight flash radiographs of the jets revealed coherent, well formed jets with jet parameters closely predicted by the a priori hydrocode calculations.




TABLE OF CONTENTS

		<u>Page</u>
	LIST OF FIGURES	v
Paragraph	1. INTRODUCTION	1
	2. THEORETICAL HEMISPHERICAL LINER STUDIES	2
	3. EXPERIMENTAL HEMISPHERICAL LINER STUDIES	12
	3.1 Fabrication	12
	3.2 Experimental tests	18
	4. THEORETICAL CONICAL LINER STUDIES	23
	5. EXPERIMENTAL CONICAL LINER STUDIES	23
	5.1 Fabrication	23
	5.2 Experimental tests	23
	6. SUMMARY AND CONCLUSIONS	29
	LIST OF REFERENCES	35
	DISTRIBUTION LIST	37

Accession For	
NTIS CRA&I	<input checked="" type="checkbox"/>
DTIC TAB	<input type="checkbox"/>
Unannounced	<input type="checkbox"/>
Justification	
By	
Distribution /	
Availability Codes	
Dist	Avail and/or Special
A-1	



FIGURES

	<u>Page</u>
FIGURE 1. Geometry of point-initiated charge	3
2. HELP code simulation of jet formation from a hemispherical liner charge for the point-initiated case at three times after detonation	4
3. Comparison of HELP and EPIC-2 computer code simulations of jet formation from a hemispherical liner charge for the point-initiated case at $t = 56\mu s$ after detonation	5
4. HELP code calculation of velocity vs time for five tracer particles at original polar angle of 30° in the point-initiated hemispherical liner	6
5. Computer code (HELP and DEFEL) simulation of jet formation of a hemispherical liner charge	7
6. HELP code simulation of jet formation from a hemispherical liner charge for the point-initiated case at $t = 76\mu s$ after detonation	8
7. DEFEL code simulation of a thick-pole tapered-wall hemispherical liner charge	9
8. Geometry of surface-initiated (implosive) hemispherical liner charge	10
9. HELP code jet geometries showing layers of tracer particles at comparable times after detonation	11
10. Cylinders used to fabricate a stratified, bimetallic disc	13
11. Final cylinder assembly for the stratified, bimetallic disc	14
12. Setup for diffusion bonding of copper-nickel assemblies (temperature $982^\circ C$, time 1 to 3 hours, argon atmosphere)	15
13. Diffusion bonded, stratified, copper-nickel cylinder	16
14. Finish machined, stratified, copper-nickel hemispherical shaped-charge liner	17
15. Free-flight flash radiographs of the jet from a stratified copper-nickel hemispherical shaped-charge liner	19
16. Recovered jet particles from a stratified copper-nickel hemispherical shaped-charge liner	20
17. Cross sections of recovered jet particles from a stratified copper-nickel hemispherical shaped-charge liner	21
18. Cross section of one half of a recovered jet particle from a stratified copper-nickel hemispherical shaped-charge liner	22
19. HELP code simulation of a 42° conical-liner charge, initial liner geometry (top), jet and slug at $40\mu s$ (center and bottom)	24
20. HELP code simulation of a 42° conical-liner charge, initial liner geometry (top), jet and slug at $60\mu s$ (center and bottom)	25
21. Diffusion bonding set up for fabricating stratified copper-nickel conical shaped-charge liners	26
22. Finish machined, stratified, copper-nickel, conical shaped-charge liner	27
23. Free-flight flash radiographs of the jet from a stratified copper-nickel conical shaped-charge liner	28
24. Jet particle from a stratified copper-nickel conical shaped-charge liner	30

FIGURES CONTINUED

	<u>Page</u>
FIGURE 25. Cross section of jet particle from a stratified copper-nickel conical shaped-charge liner	31
26. Central region of jet particle from a stratified copper-nickel conical shaped-charge liner	32
27. Recovered slug from a stratified copper-nickel conical shaped- charge liner	33

1. INTRODUCTION

Analytical studies regarding the liner collapse and jet formation of hemispherical warheads were published in 1985 by Chou, Walters, Ciccarelli, and Weaver¹, hereafter designated as CWCW. This analysis revealed the so-called "tubular-layer" formation process for point-initiated, hemispherically lined shaped-charge warheads. The "tubular-layer" formation process states that each liner element stretches across its thickness into a tubular jet, similar to an extrusion process. The HELP and the EPIC-2 computer codes both predicted this formation process and were in general agreement regarding the final jet properties as well as the jet formation process.

Also, hemispherical liners driven by an implosive detonation, i.e., a surface-initiated hemispherical shaped-charge revealed a different collapse and jet formation process. The collapse and formation of conical shaped-charge warheads was also studied analytically in the CWCW report.¹

The a priori computer code predictions suggested a method to verify the "tubular layer" formation theory. As in the hydrocode calculations, a stratified, bimetallic hemispherical liner was fabricated. The alternating layers of material, namely copper and nickel, were joined by a diffusion bond. Copper and nickel were chosen because of their similarity under shock loading conditions, identical densities and ease of diffusion bonding.^{3,4} A cylinder of alternating discs of copper and nickel was first fabricated by diffusion bonding and then conical and hemispherical liners were machined from the cylinder forming the stratified, bimetallic liners.

Both the conical and hemispherical liners were loaded with 75/25 Octol, point-initiated, and fired into air to obtain free-flight flash radiographs. Both the conical and hemispherical warheads were also fired into water and typically, two or three intact jet particles were recovered. For the conical warhead, the slug was also recovered. The recovered particles, and the slug, were cross sectioned and analyzed to reveal the flow pattern of the copper and the nickel. The cross sectioned jet particles tend to substantiate the hydrocode analyses.

Previous studies regarding the collapse and jet formation process of conical liners were conducted by Perez, et al.² In their experiments, a conical liner consisting of a copper region near the apex of the cone, a brass region along the middle of the slant height of the cone, and a copper region near the base of the cone was tested. This conical liner is, in effect, a three layer, stratified, bimetallic liner. The main conclusion from Perez, et al.², in reference to the slug recovered from this liner, is stated as follows: "The slug is originated from a superimposition process of its own elements. Except for the first liner elements, the collapse occurs off the axis and on the previously imploded liner material."² This implies a "layering" of jet material akin to a "tubular formation" process. However, the slug recovered by Perez, et al. and the slug recovered in this study do not reveal identical flow patterns.

The remainder of this report will describe the method of fabrication of stratified, bimetallic liners, and present the experimental test results. The tests consist of free-flight flash radiographs and liner particles recovered by firing into water.

2. THEORETICAL HEMISPHERICAL LINER STUDIES

The collapse and jet formation process for shaped-charges with hemispherical liners were studied in the CWCW report.¹ Both the HELP and the EPIC-2* computer codes predicted a "tubular-layered" collapse of the hemispherical liner elements for a point-initiated shaped-charge with a hemispherical liner. Details of this study are given by CWCW and only a few highlights will be repeated here.

The basic charge geometry is shown in Figure 1. Figure 2 illustrates the liner collapse as simulated by the HELP code. The original liner was modeled as a stratified, bimetallic liner of two materials with identical material properties. This was accomplished by using massless tracer particles to differentiate between the two materials. Figure 3 delineates the comparison between the Eulerian code HELP and the LaGrangian code EPIC-2.* The two codes are in excellent qualitative agreement with respect to the jet formation process. This agreement is fortunate since EPIC-2 or DEFEL runs faster and is less expensive than the HELP code. The "tubular-layered" jet formation process for a point-initiated, uniform wall thickness, hemispherical liner is illustrated in Figures 2 and 3. Again, the details are given in CWCW.¹

Figure 4 depicts the usage of the massless tracer particles. In this case, the velocities of five interior points through the liner wall are monitored and plotted as a function of time. Figure 5 illustrates the application of the massless tracer particle technique to the tracking of each region of the liner for the stratified, bimetallic, hemispherical liner. Figure 6 shows the complete formation of this liner.

Figure 7 shows a similar code calculation for a tapered hemispherical liner with the pole thickness equal to twice the equatorial or rim thickness. For a point-initiated charge, a "tubular-layered" jet formation still occurs. However, for a surface-initiated hemispherical liner the jet collapse and formation process is quite different. Figure 8 presents the initial surface-initiated charge geometry. Figure 9 reveals the differences in jet collapse and formation between the two modes of initiation.

The analyses presented above suggested a way in which hemispherical shaped-charge liners collapsed, with the collapse and formation depending on the mode of initiation. Thus, an attempt was made to experimentally verify the results of the CWCW report¹, as outlined above.

* Or DEFEL, the Dyna East modified version of EPIC-2.

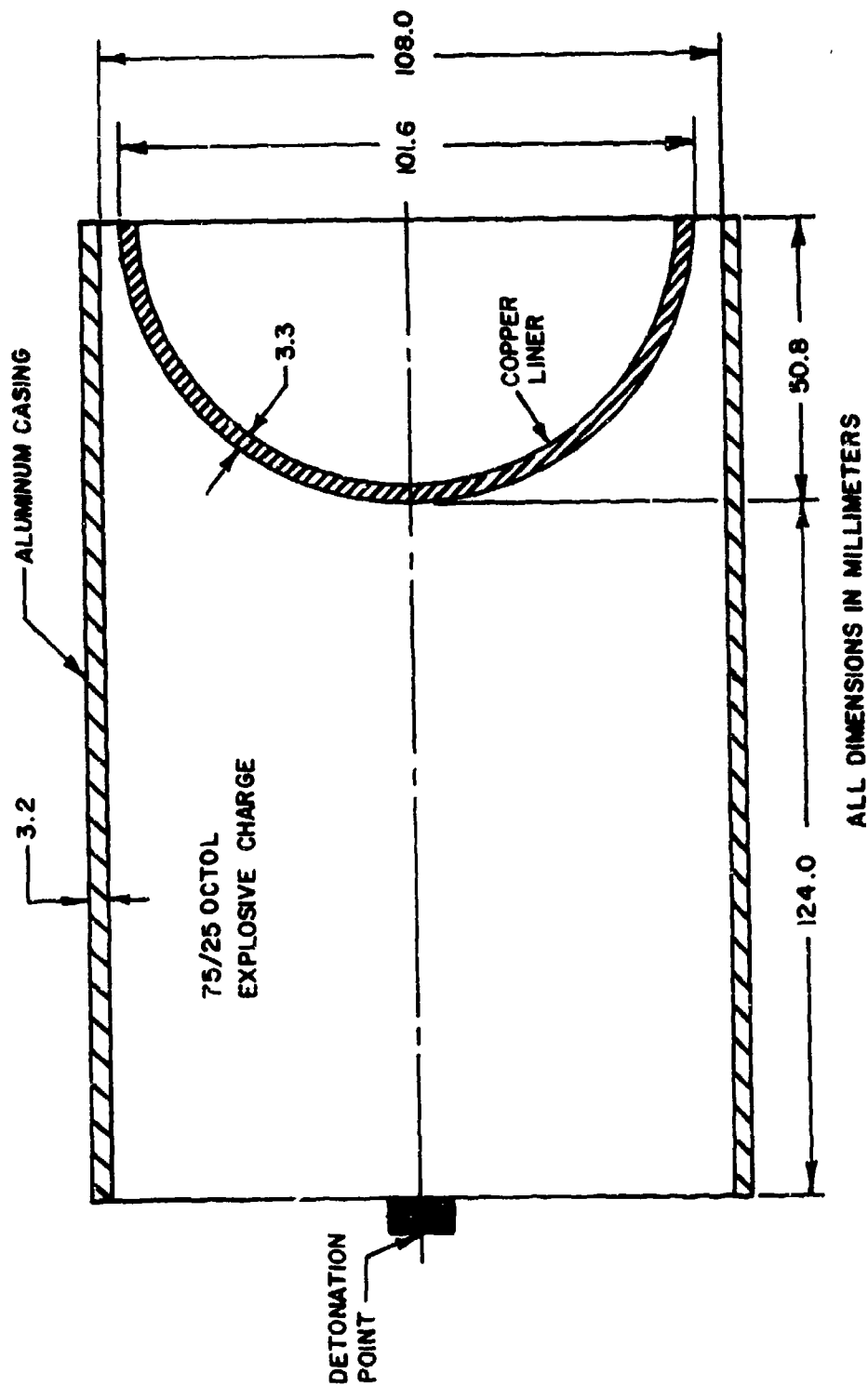


Figure 1. Geometry of point-initiated charge.

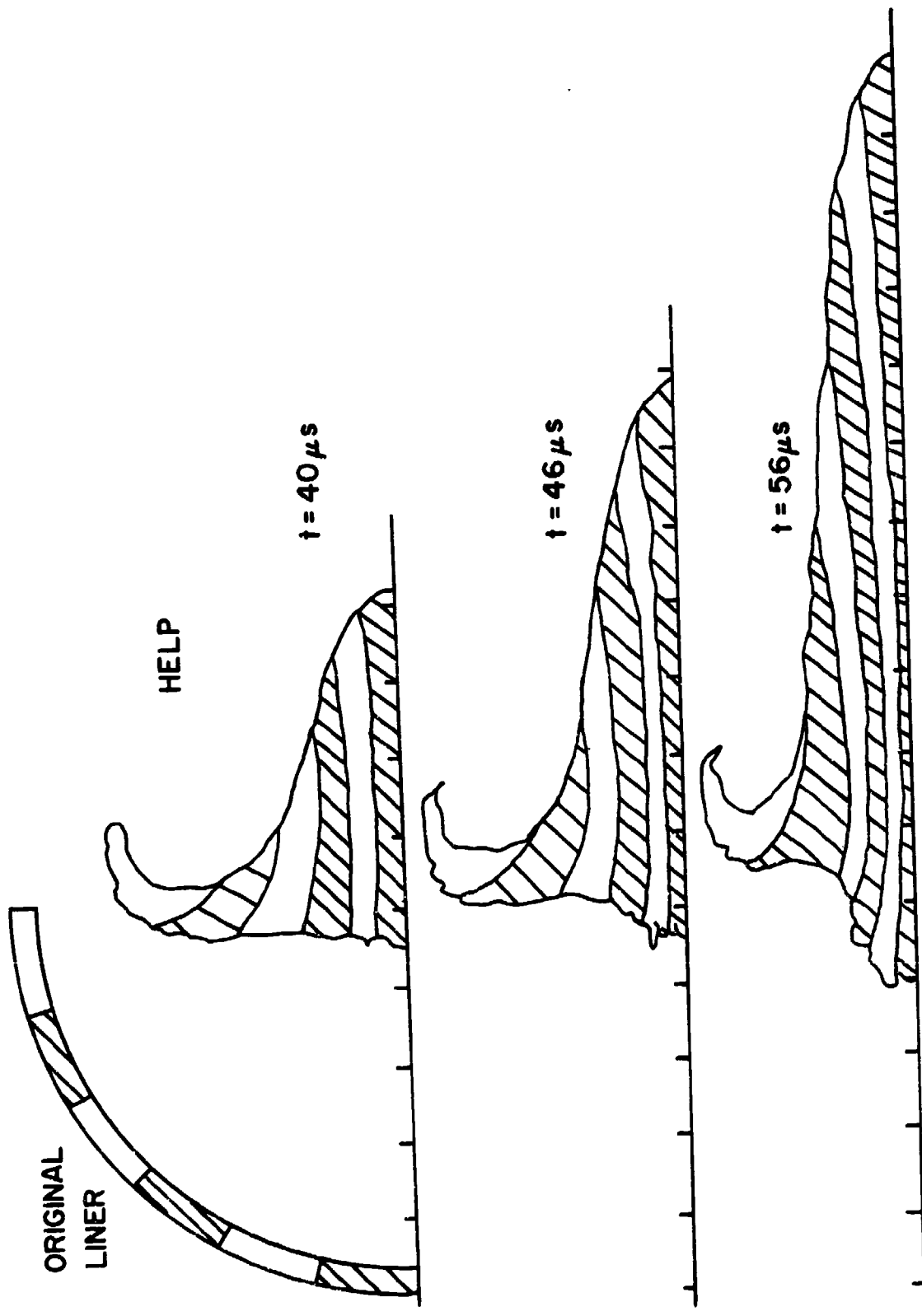


Figure 2. HELP code simulation of jet formation from a hemispherical liner charge for the point-initiated case at three times after detonation.

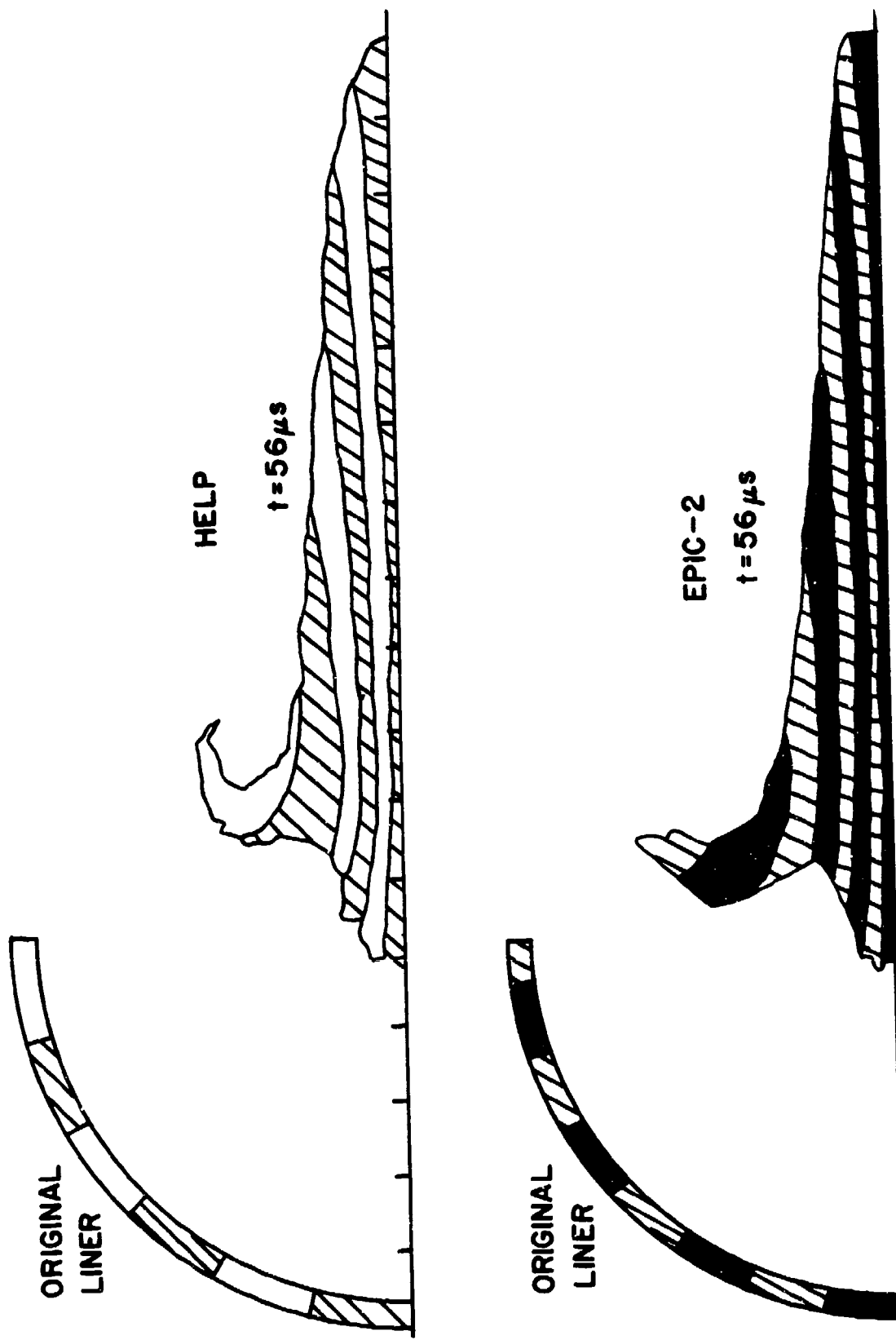


Figure 3. Comparison of HELP and EPIC-2 computer code simulations of jet formation from a hemispherical liner charge for the point-initiated case at $t=56\mu s$ after detonation.

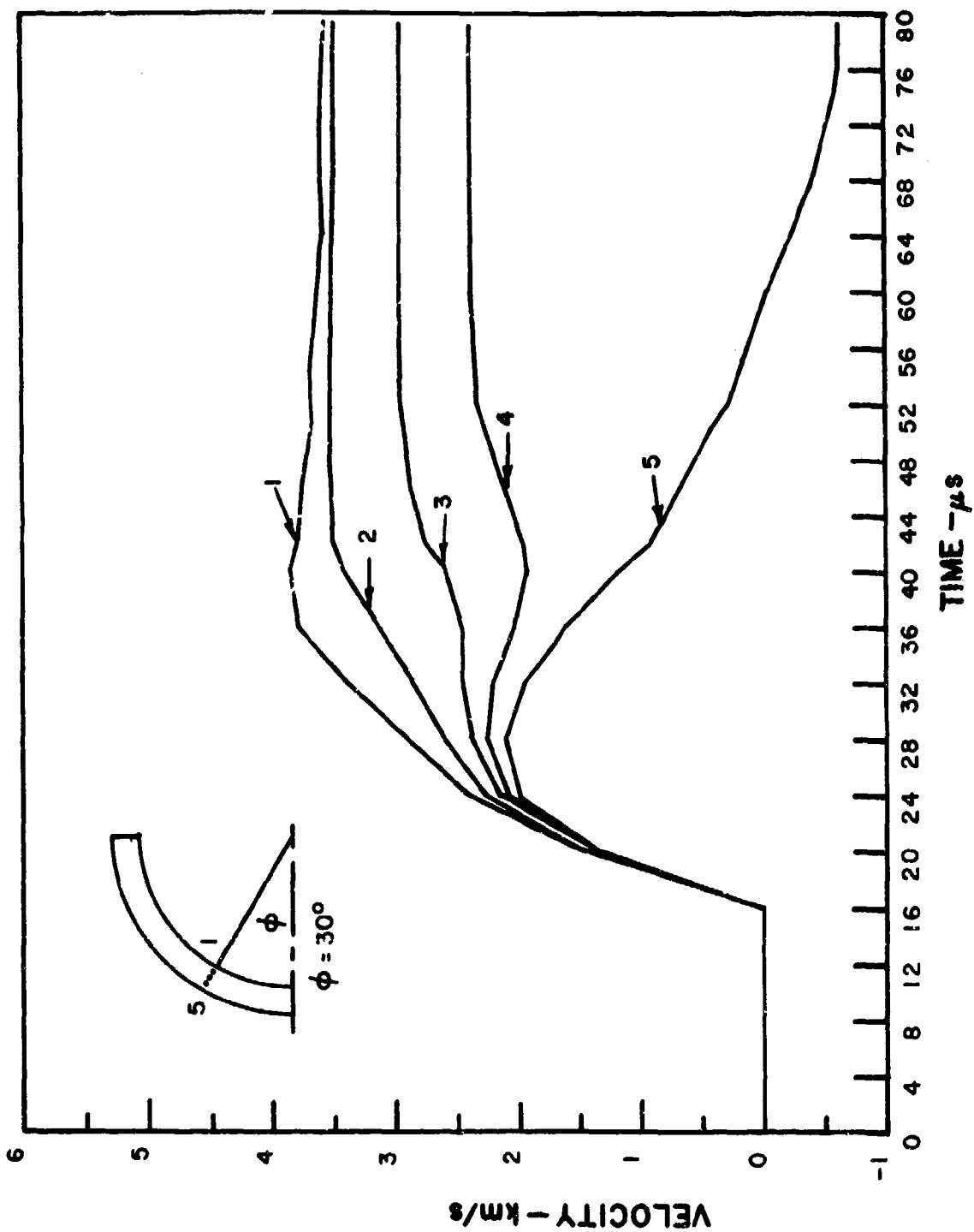


Figure 4. HELP code calculation of velocity vs. time for five tracer particles at original polar angle of 30° in the point-initiated hemispherical liner.

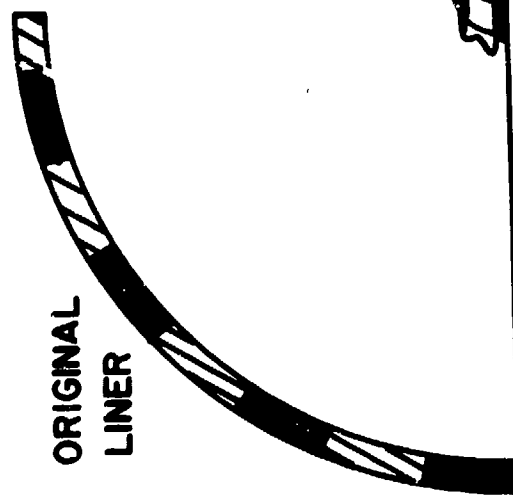
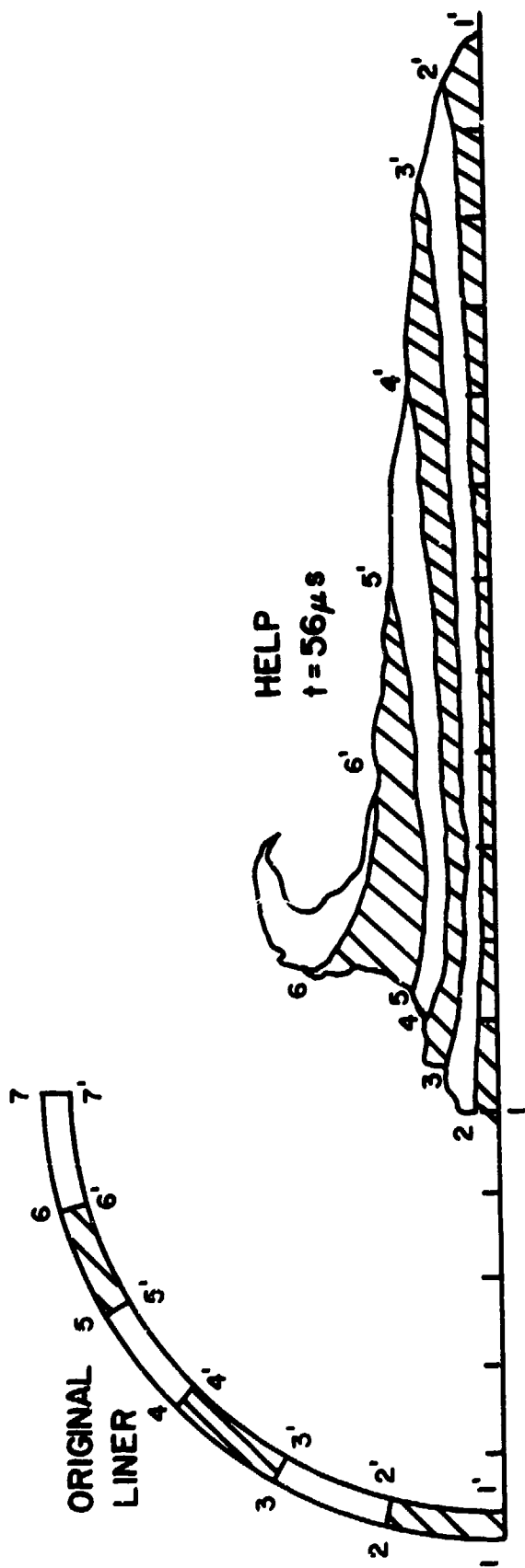


Figure 5. Computer code (HELP and DEFEL) simulation of jet formation of a hemispherical liner charge.

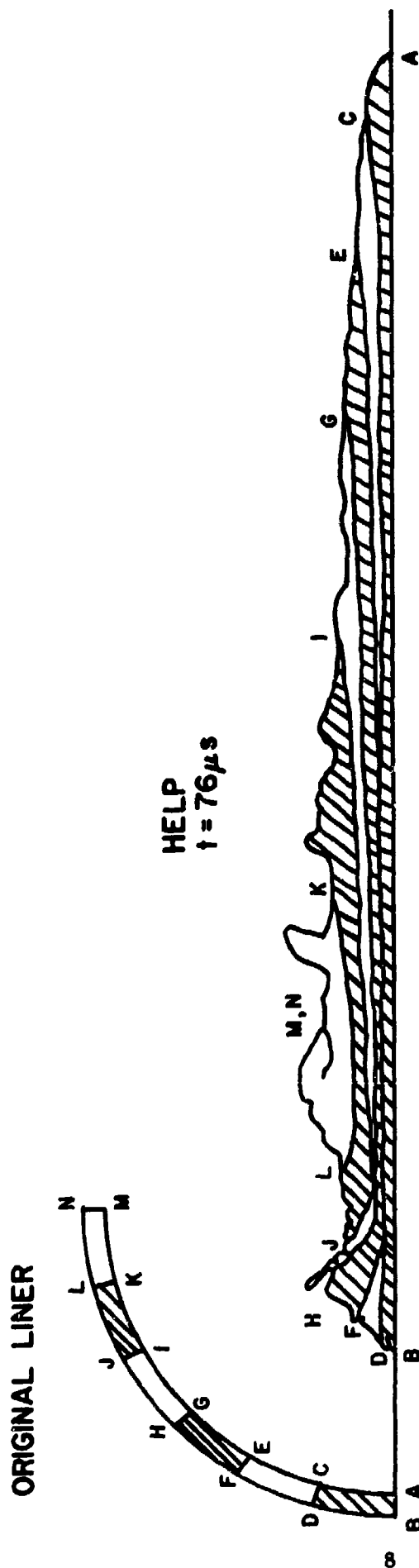
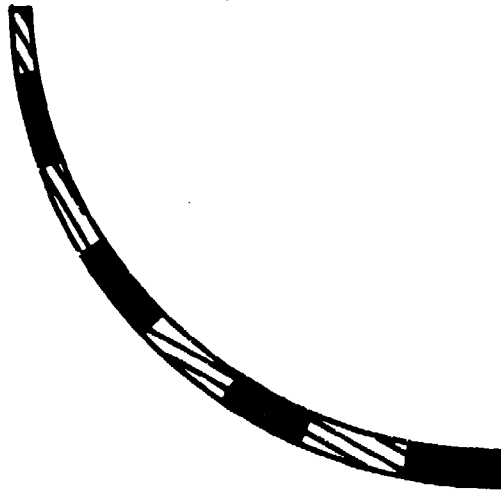


Figure 6. HELP code simulation of jet formation from a hemispherical liner charge for the point-initiated case at $t = 76 \mu s$ after detonation.

ORIGINAL LINER



$$\frac{\text{POLE THICKNESS}}{\text{RIM THICKNESS}} = 2$$

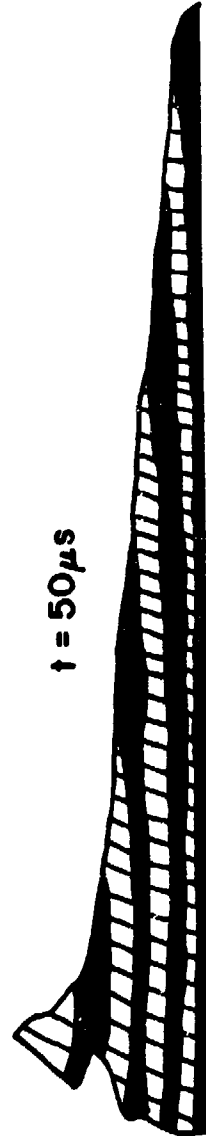


Figure 7. DEFEL code simulation of a thick-pole tapered-wall hemispherical liner charge.

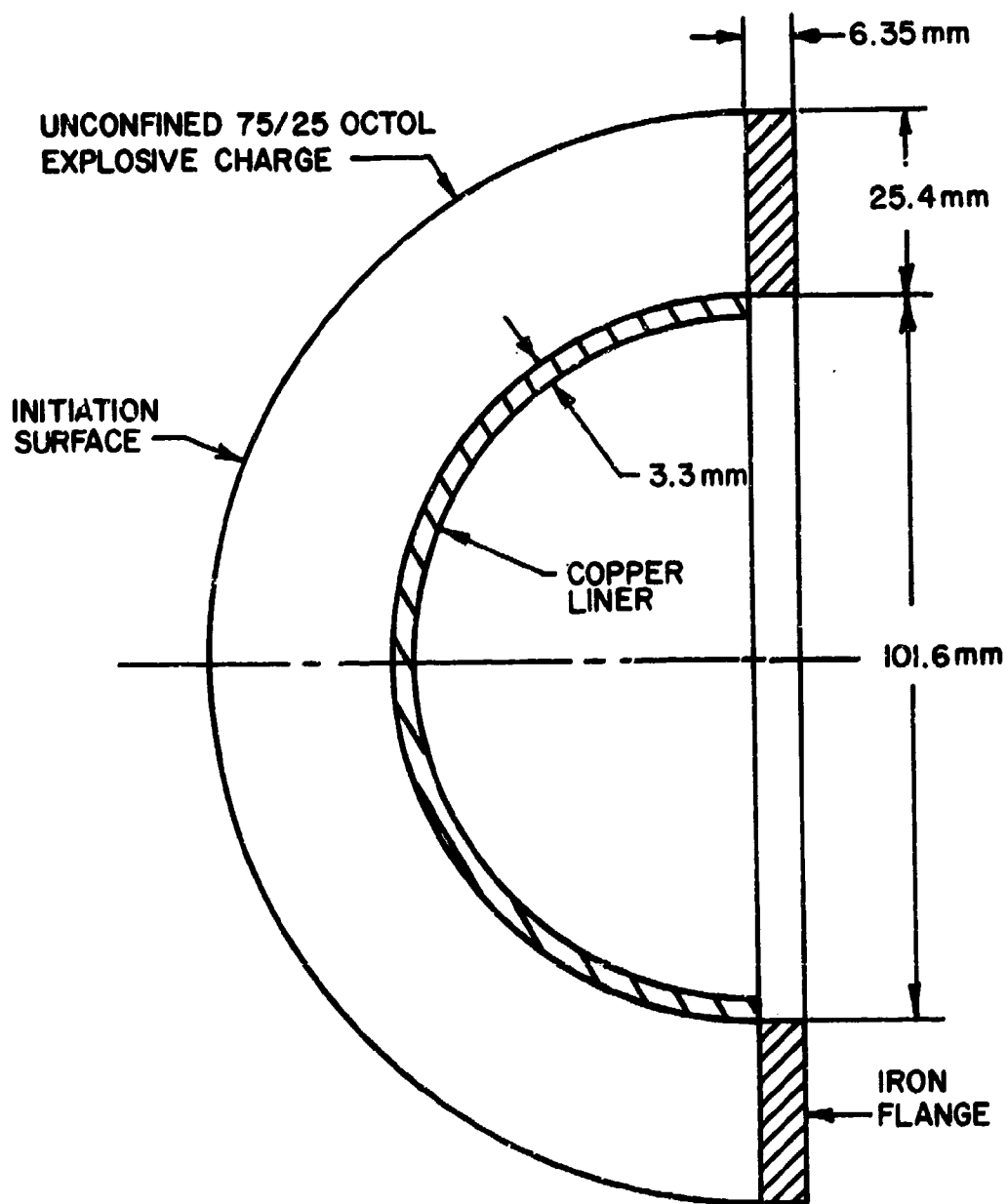


Figure 8. Geometry of surface-initiated (implosive) hemispherical liner charge.

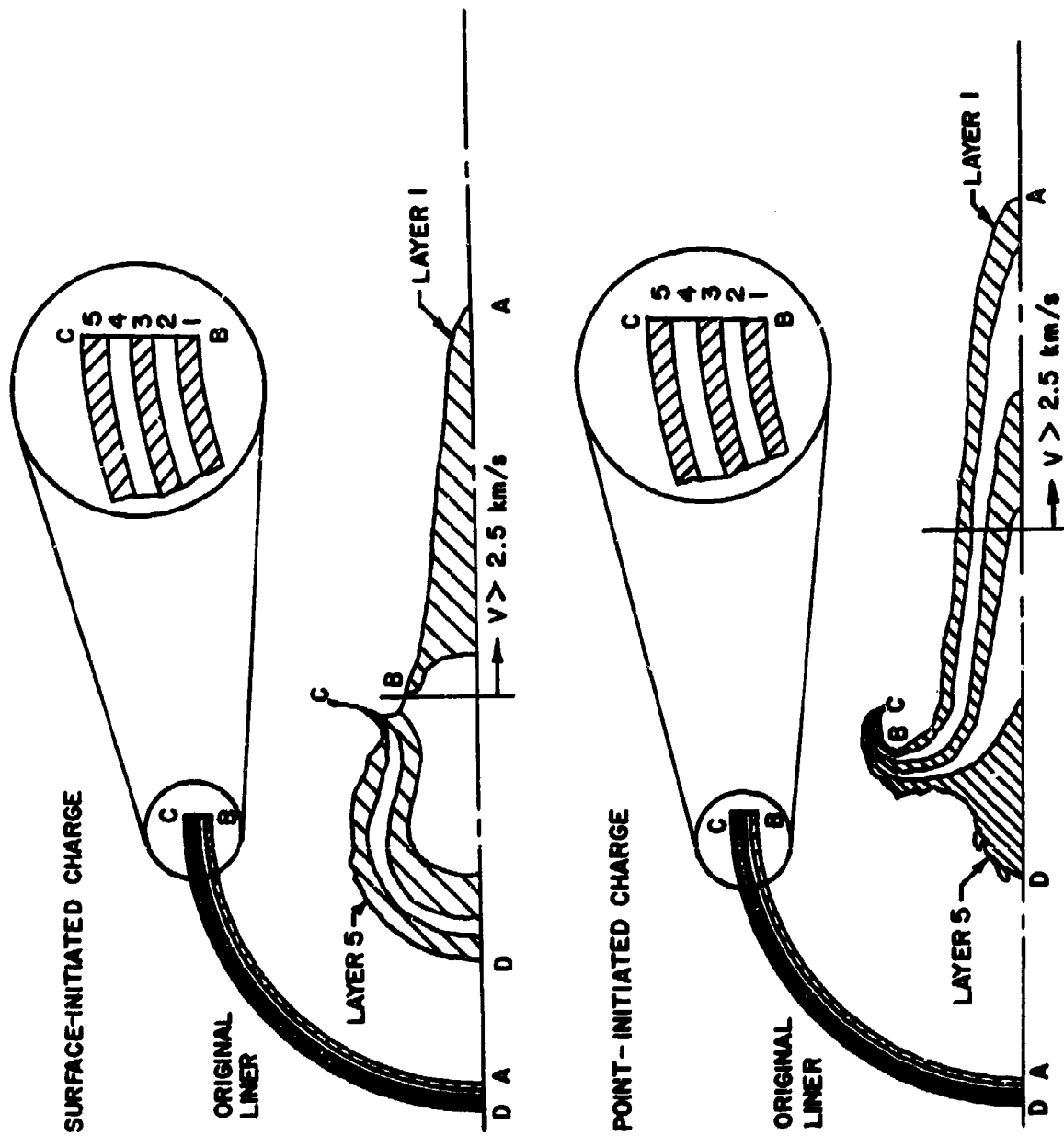


Figure 9. HELP code jet geometries showing layers of tracer particles at comparable times after detonation.

3. EXPERIMENTAL HEMISPHERICAL LINER STUDIES

3.1 Fabrication. The experimental study involved fabricating a stratified, bimetallic liner. It was decided that the two materials to be used in the liner would be copper and nickel due to their identical density and similar behavior under shock loading conditions. It remained to devise a way to attach the two materials.

One possible approach would be to form a series of cylinders or rods, all but the smallest of which were hollow. The solid rod, say of copper, would be placed inside a hollow rod, say of nickel. This assembly would then be placed inside a larger hollow rod of copper, and so on, until the top view of the cylinder consisted of concentric circles of alternating layers of material. Figure 10 shows the various cylinders and Figure 11 shows the final assembly including the top view. The cylinders would be assembled using a press fit and then allowed to adhere to each other by diffusion bonding. Next slice (disc) would be sawed off and the disc would be hydroformed or pressed to the final geometry. This method of fabrication, although interesting, would seem to be difficult to implement. For this reason, it was not pursued further.

Instead, the actual liners were fabricated from circular discs of copper and nickel 3.2 mm (0.125") thick. Alternate layers of these copper and nickel discs, 54 mm (2.125") in diameter were stacked up to form a cylinder 35 mm (1.375") high. The copper and nickel discs were polished and etched to present smooth clean surfaces. The cylinder of alternating discs of copper and nickel was then inserted in a loading fixture as shown in Figure 12. The loading fixture held the discs together under pressure. It was shown by Barnes and Mazey⁵ that a smooth, void free bond could be formed at a copper-nickel interface if a minimum stress of 10.34 MPa (1500 psi) was applied during the diffusion bonding. Mica was used to separate the fixture from the discs to prevent bonding the entire assembly together. The assembly was then placed in a controlled argon atmosphere furnace at 982° C (1800° F) for 1 to 3 hours to allow a diffusion bond to form between the copper-nickel discs. (A metallurgical examination of a test stack of copper-nickel discs, bonded using the above fixture, showed virtually no voids at the interfaces indicating that the fixture exerted sufficient force to apply the required stress.)

A hemispherical liner was machined from this first stack of bonded discs. During the final stages of machining, two interfaces began to debond. The time interval for bonding this first hemispherical liner was given as 1 to 3 hours because it was necessary to rebond this liner a second and third time. A special loading fixture was devised for this purpose. Subsequent stacks of discs, prior to assembly into the loading fixture, were placed in a 150 ton hydraulic press and squeezed together with sufficient force to exceed the yield stress of the copper. This caused sufficient metal flow to intimately mate the surfaces together. The net result of this high stress treatment was that bonding could be accomplished with a single one hour treatment, no further debonding occurred during final machining and the surface finish requirement was not as stringent. Overall efficiency and economy of liner manufacture was increased significantly.

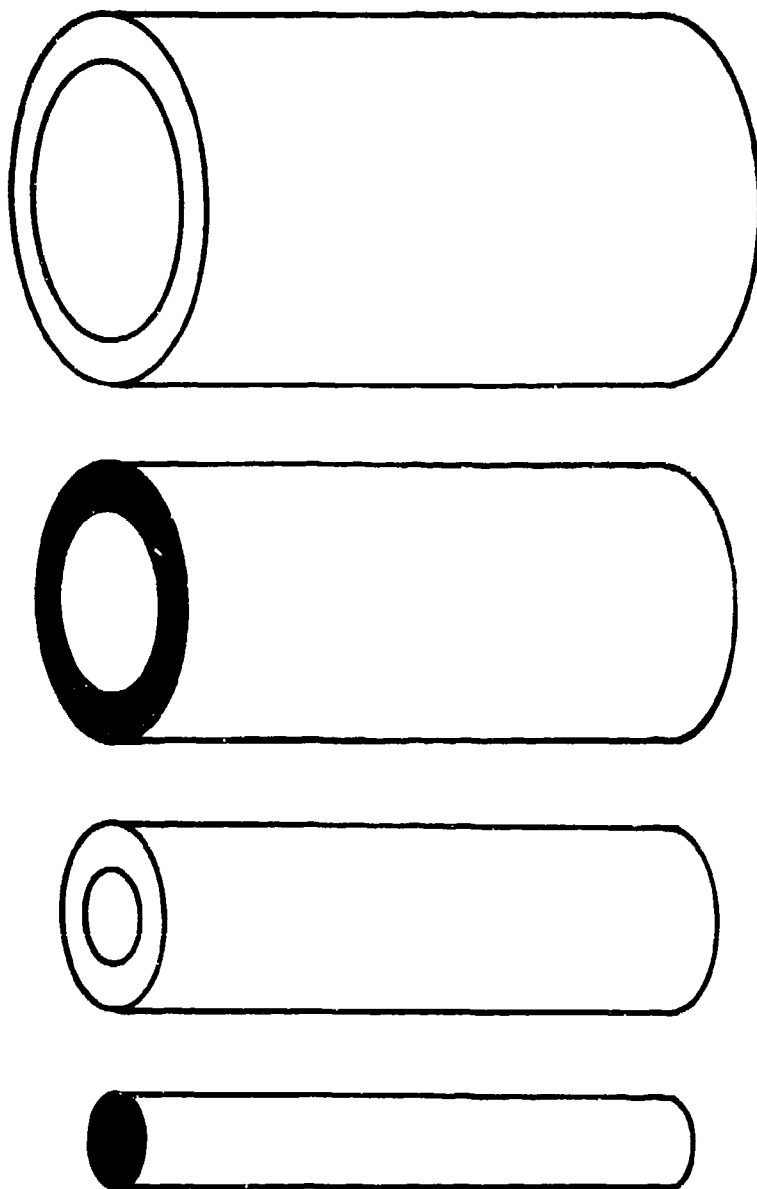


Figure 10. Cylinders used to fabricate a stratified, bimetallic disc.

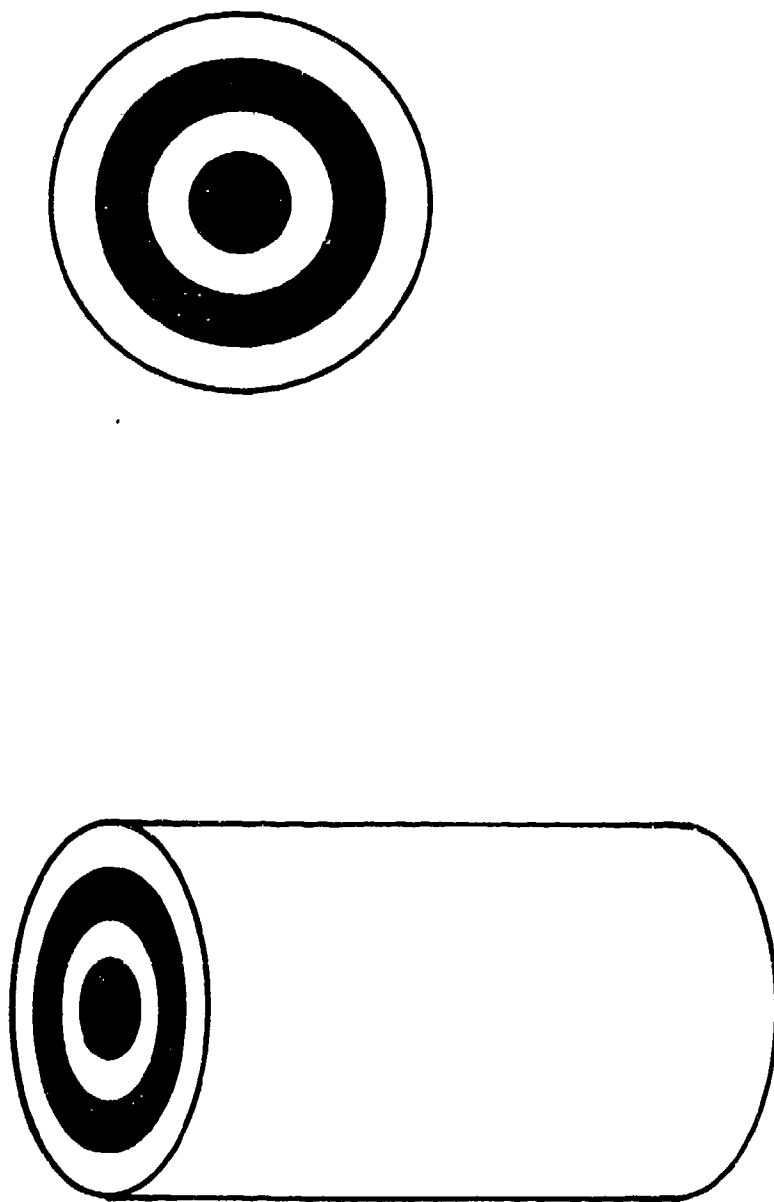


Figure 11. Final cylinder assembly for the stratified, bimetallic disc.

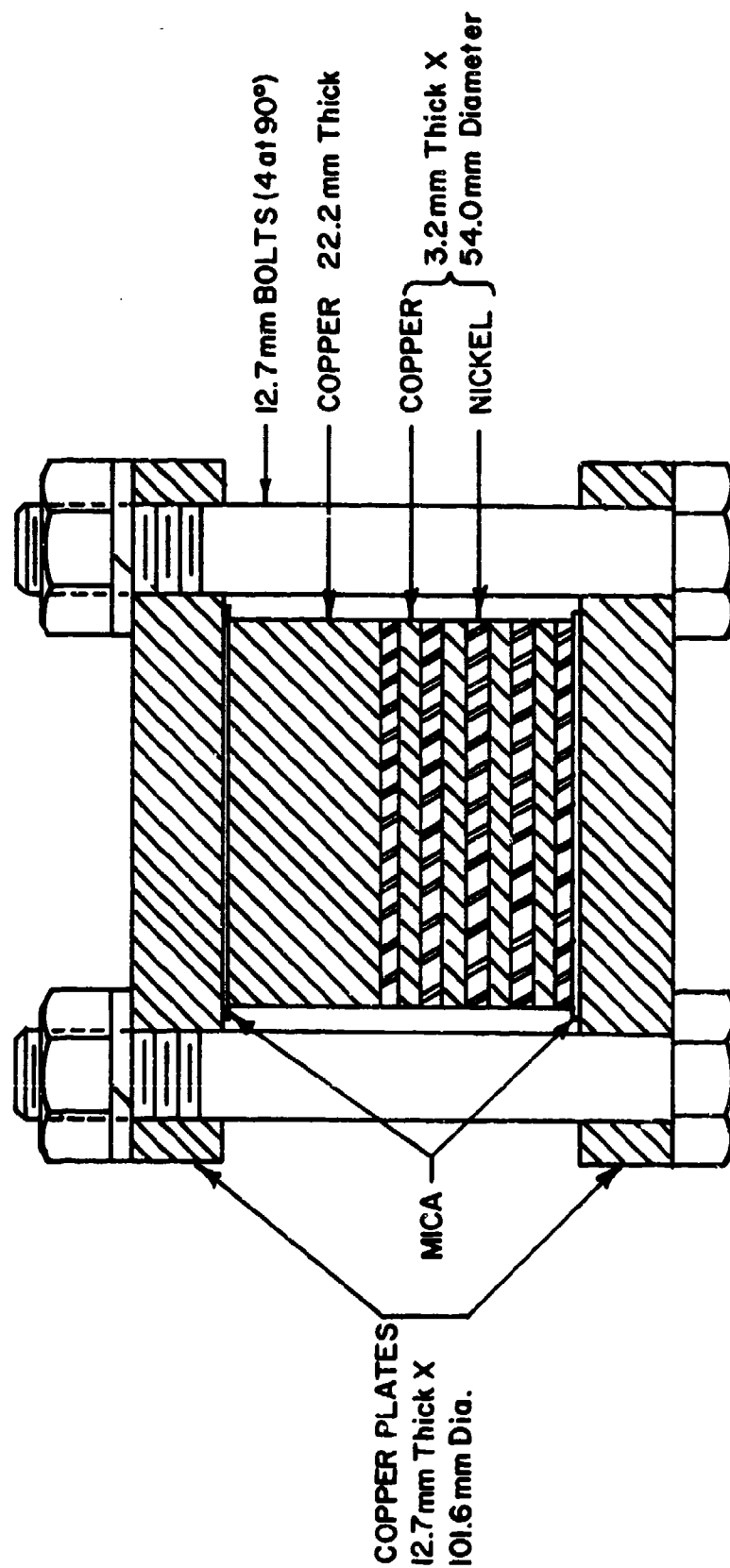


Figure 12. Setup for diffusion bonding of copper-nickel assemblies.
 (Temperature - 982 C, time 1 to 3 hours, argon atmosphere)

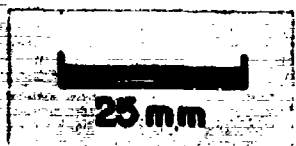
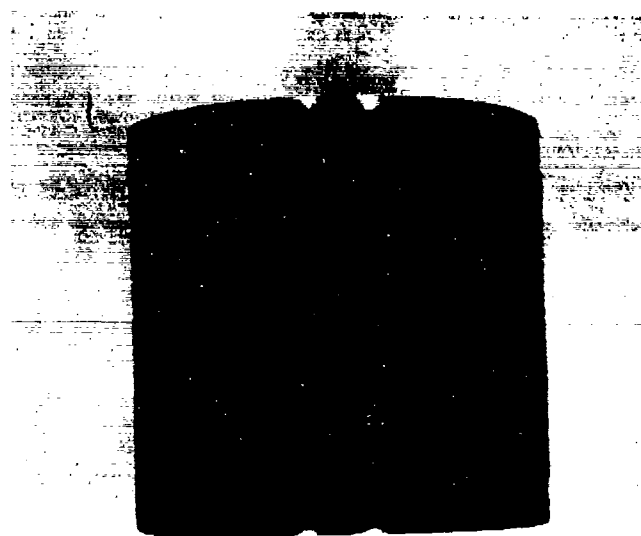


Figure 13. Diffusion bonded, stratified, copper-nickel cylinder.

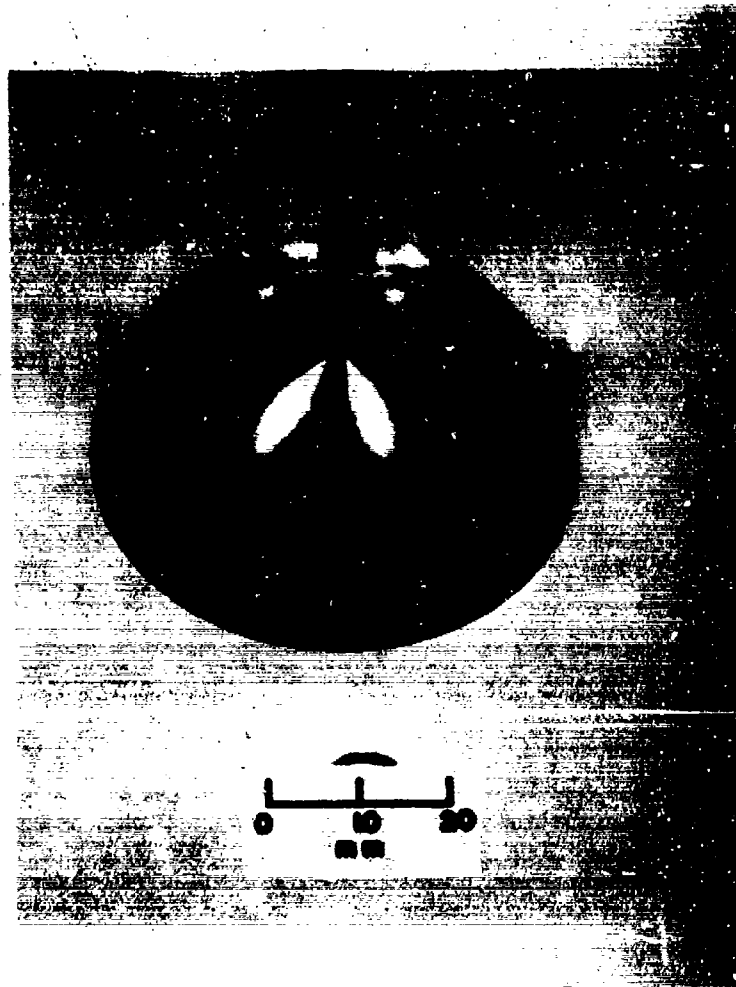


Figure 14. Finish machined, stratified, copper-nickel hemispherical shaped-charge liner.

Another technique, in lieu of diffusion bonding, would be to explosively weld the layers together to form the final assembly. This technique was not considered in this study.

The final assembly, held together by a diffusive bond is shown in Figure 13. The final liner is shown in Figure 14 and consists of nine layers with nickel at the pole and equator. The liner had an outside diameter of 54 mm (2.125") and a uniform wall thickness of 1.6 mm (0.063").

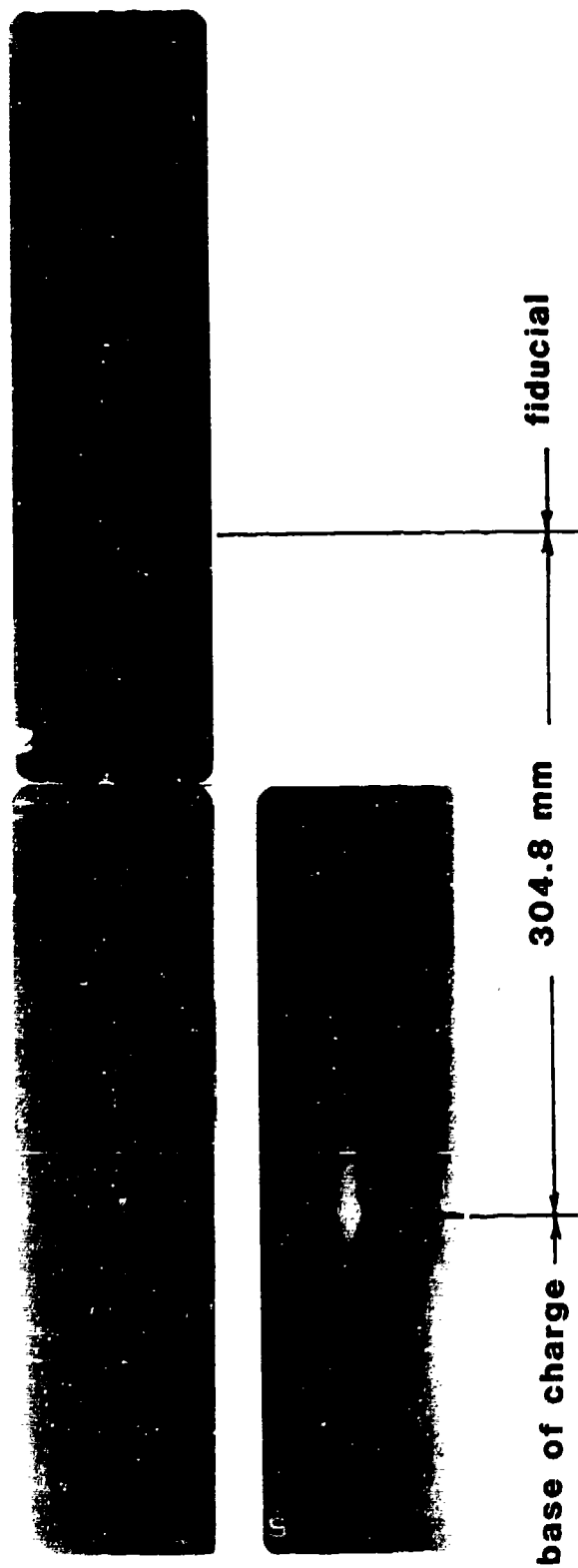
3.2 Experimental tests. The stratified, bimetallic, hemispherical liner was loaded with 75/25 Octol and housed in a thin aluminum cylinder 76.2 mm (3.0") high. The free-flight flash radiographs are shown in Figure 15 for flash times of 35.5 and 128.8 μ s. The shaped-charge formed a fairly good jet. The particles are not uniform in size and do not appear to be as ductile or as well aligned as a single material hemispherical shaped-charge with a copper or nickel liner. Also, the jet breakup appears to be early. Nonetheless, the copper-nickel stratified interfaces did not preclude jetting. The penetration into RHA (Rolled Homogeneous Armor) was 29 mm (1.125") at a 1.47 m (58.0") standoff-distance.

Two water recovery tests were conducted. In the first, the liner was fired with a reduced head height (i.e., the total charge height was 38.1 mm (1.5")) into a water column with a 457 mm (18.0") standoff-distance. A few particles were recovered.

The second particle recovery test used the full head height charge and was fired into a water column at a standoff-distance of 254 mm (10.0"). This technique resulted in more recovered particles of better quality (i.e., longer) than in the reduced head height test and will be used in future tests. The recovered particles from this test were cross sectioned.

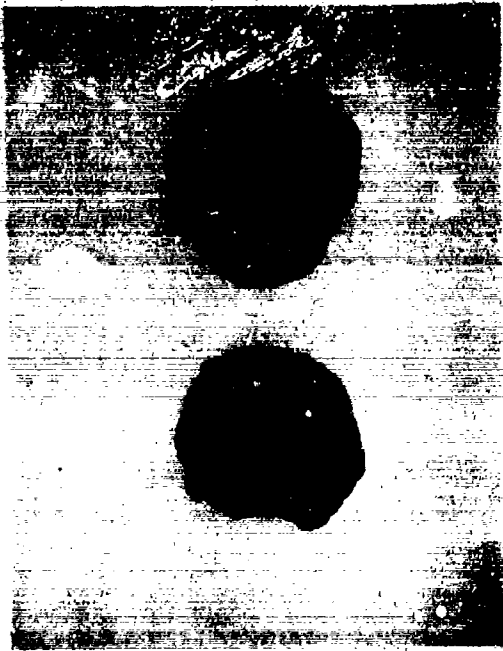
Figure 16 shows the top and side views of the two largest particles recovered in this test. Both copper and nickel are present. Figure 17 shows a cross section of these particles. Both copper and nickel are again present and in alternating layers. A cross section of the left particle in Figure 17, in a direction orthogonal to the first cut, is shown in Figure 18. Again, alternate layers of copper and nickel are present. Note that nine alternating layers of material are visible which corresponds to the nine original layers of material visible in Figure 14. This layered pattern of jet material verifies, at least in part, the "tubular-layer" jet collapse and formation theory discussed earlier.

The collapse and formation theory for point-initiated, hemispherical, shaped-charge warheads is not completely verified since only a few particles were recovered. The recovered particles probably were located near the rear of the jet since the particles near the front of the jet were probably eroded away while penetrating the water column at hypervelocity. Thus, we have no guarantee that all jet particles would reveal the same tubular, layered flow pattern. Obviously, a better technique to recover shaped-charge jet particles would be advantageous.



times 35.5 and 128.8 μ sec.

Figure 15. Free-flight flash radiographs of the jet from a stratified copper-nickel hemispherical shaped-charge liner.



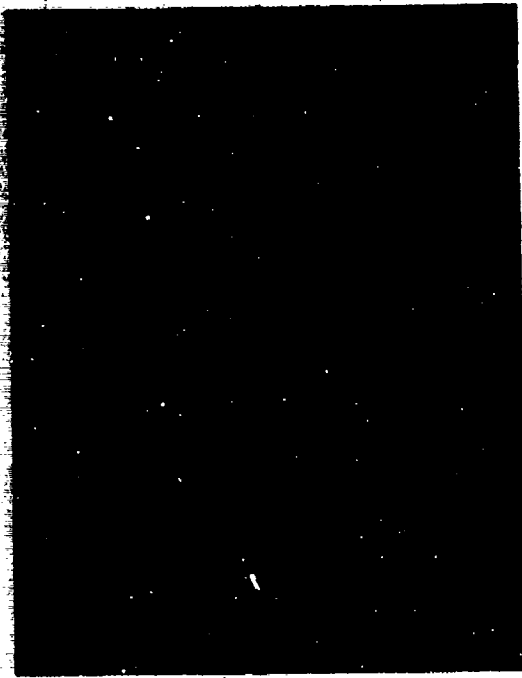
TOP VIEW

1.0cm



SIDE VIEW

Figure 16. Recovered jet particles from a stratified copper-nickel hemispherical shaped-charge liner.



1.0 cm

Figure 17. Cross sections of recovered jet particles from a stratified copper-nickel hemispherical shaped-charge liner.



50X MAGNIFICATION

Figure 18. Cross section of one half of a recovered jet particle from a stratified copper-nickel hemispherical shaped-charge liner.

4. THEORETICAL CONICAL LINER STUDIES

The same numerical technique, i.e., a HELP code calculation, was used to investigate the flow pattern of a conical, stratified, bimetallic liner. This study was deemed appropriate because hemispherical and conical shaped-charge liners undergo different collapse and jet formation processes.

The initial conical liner is shown in Figure 19. The liner had an outside diameter of 101.6 mm (4.0"), an apex angle of 42° , and an uniform wall thickness of 3.3 mm (0.13"). The explosive cylinder had a diameter of 108 mm (4.25") and the head height was 42.46 mm (1.67"). The explosive fill was 75/25 Octol and was point-initiated. Figures 19 and 20 illustrate the collapse and formation of the conical liner at 40 and 60 μ s, respectively. Note that the conical liner undergoes a jetting or flow splitting process. Further analytical details are given in the CWCW¹ report. Experimental studies with stratified, bimetallic, conical liners were conducted in an attempt to verify these analytical results.

5. EXPERIMENTAL CONICAL LINER STUDIES

5.1 Fabrication. The stratified, bimetallic, conical liners were fabricated by diffusion bonding stacks of wide angle (120°), 5 mm (0.197") thick, alternately layered copper-nickel cones. The diffusion bonding procedure and conditions were the same as was used for the final hemispherical liners. The test setup and final liner dimensions are depicted in Figure 21. The liner had an outside diameter of 50 mm (1.97"), a uniform wall thickness of 1.27 mm (0.05") and an apex angle of 60° . Figure 22 shows the final machined liner with 9 layers of materials.

5.2 Experimental tests. The stratified, bimetallic, conical liner was loaded with Composition B and point-initiated with a one liner diameter head height. The explosive fill was confined in a thin aluminum body. The free-flight flash radiograph is shown in Figure 23.

The flash times were 81.3, 126.2 and 170.0 μ s. The jet is of good quality and exhibits no evidence of interference between the two materials. The jet particles are regular in shape and not well aligned. The penetration into RHA was 1.75" at a 1.52 m (60.0") standoff-distance.

The water recovery test entailed firing the stratified, bimetallic, conical shaped-charge into a water column at a 609.6 mm (24.0") standoff-distance. The slug was recovered in good condition. The apex end of the slug apparently hit the side of the gun tube used to hold the water column and was slightly deformed. In addition to the slug, several small jet particles were recovered.

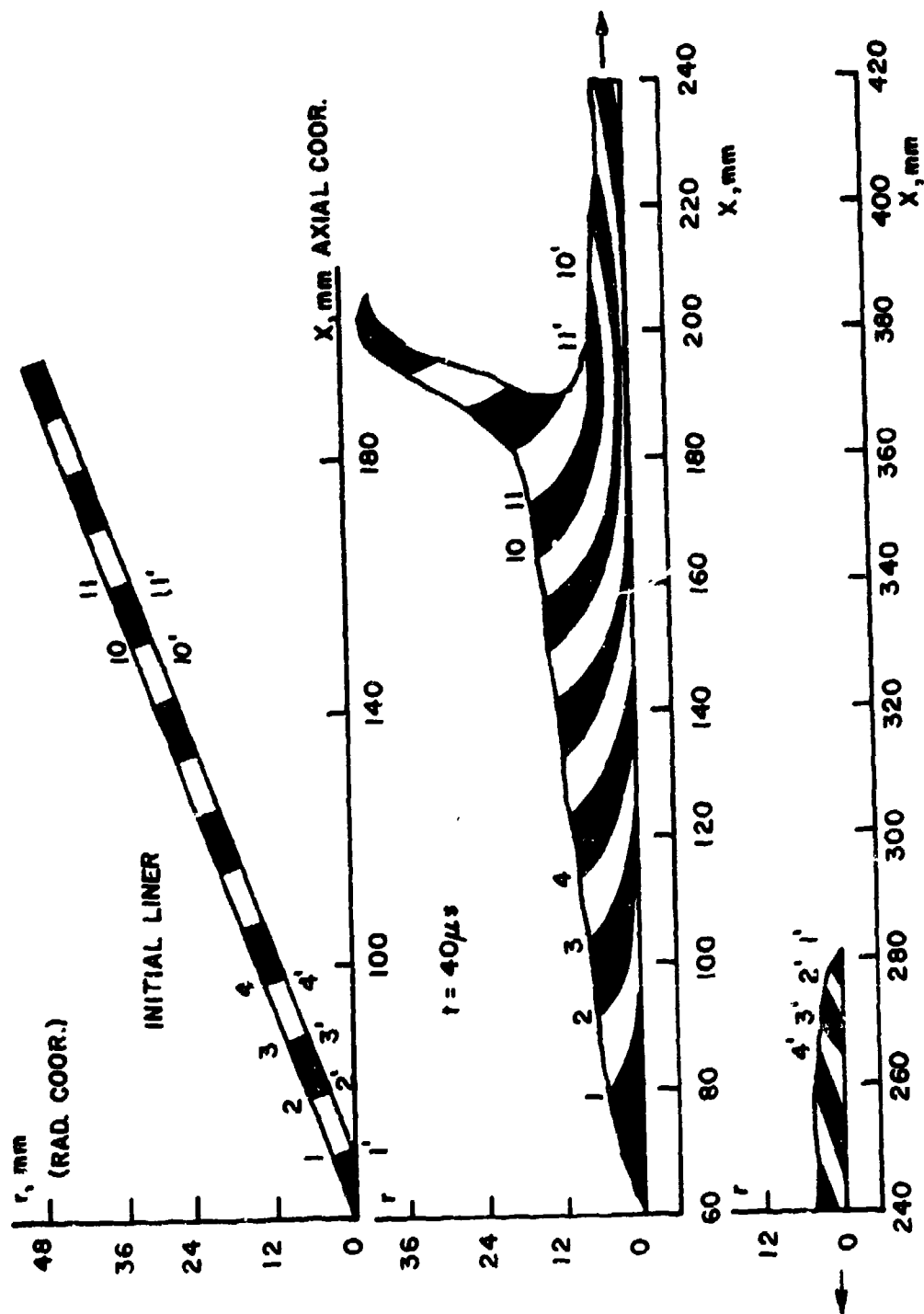


Figure 19. HELP code simulation of 42° conical-liner charge, initial liner geometry (top), jet and slug at 40 μ s (center and bottom).

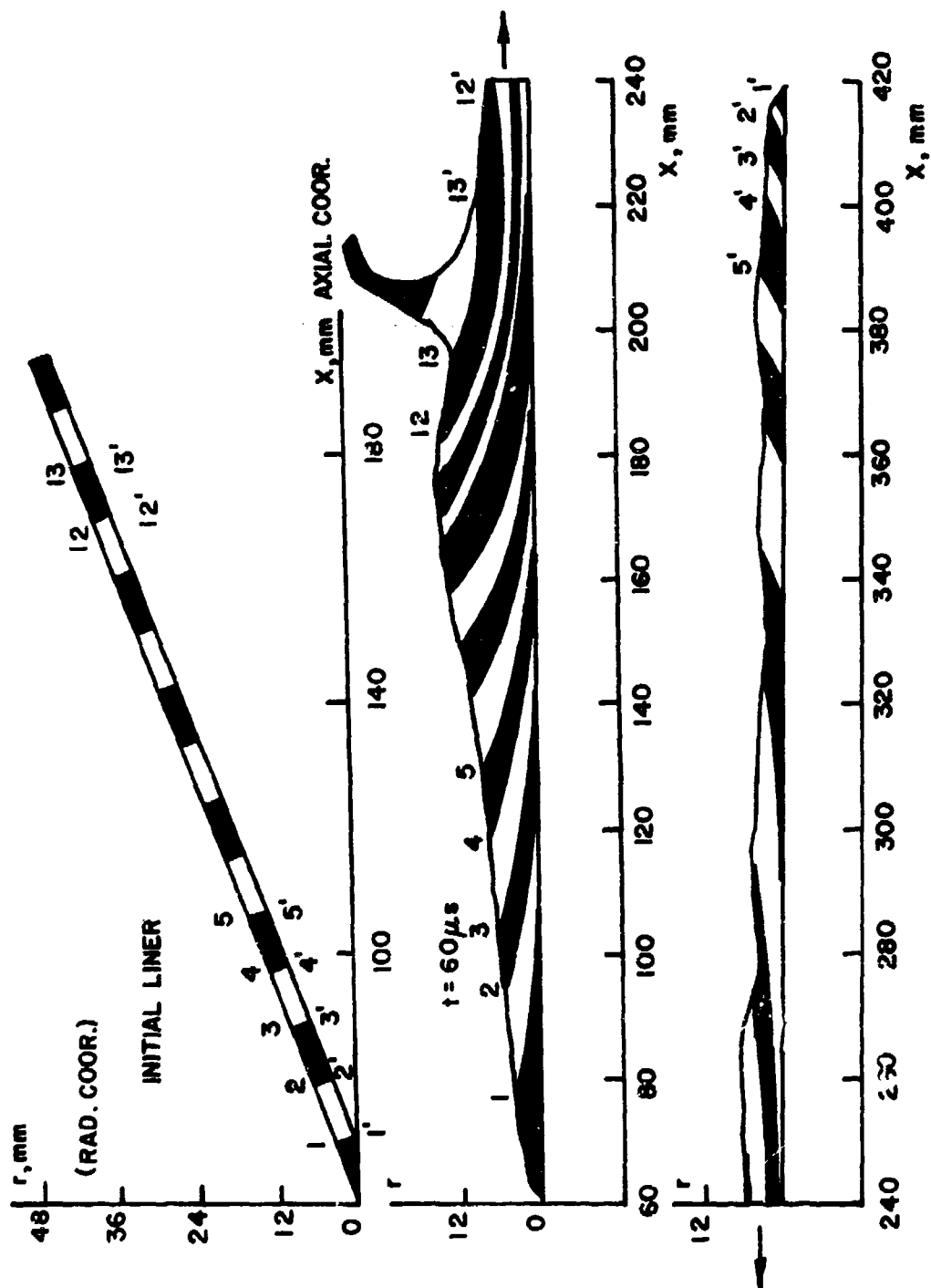


Figure 20. HELP code simulation of a 42° conical-liner charge, initial liner geometry (top), jet and slug at 60μs (center and bottom).

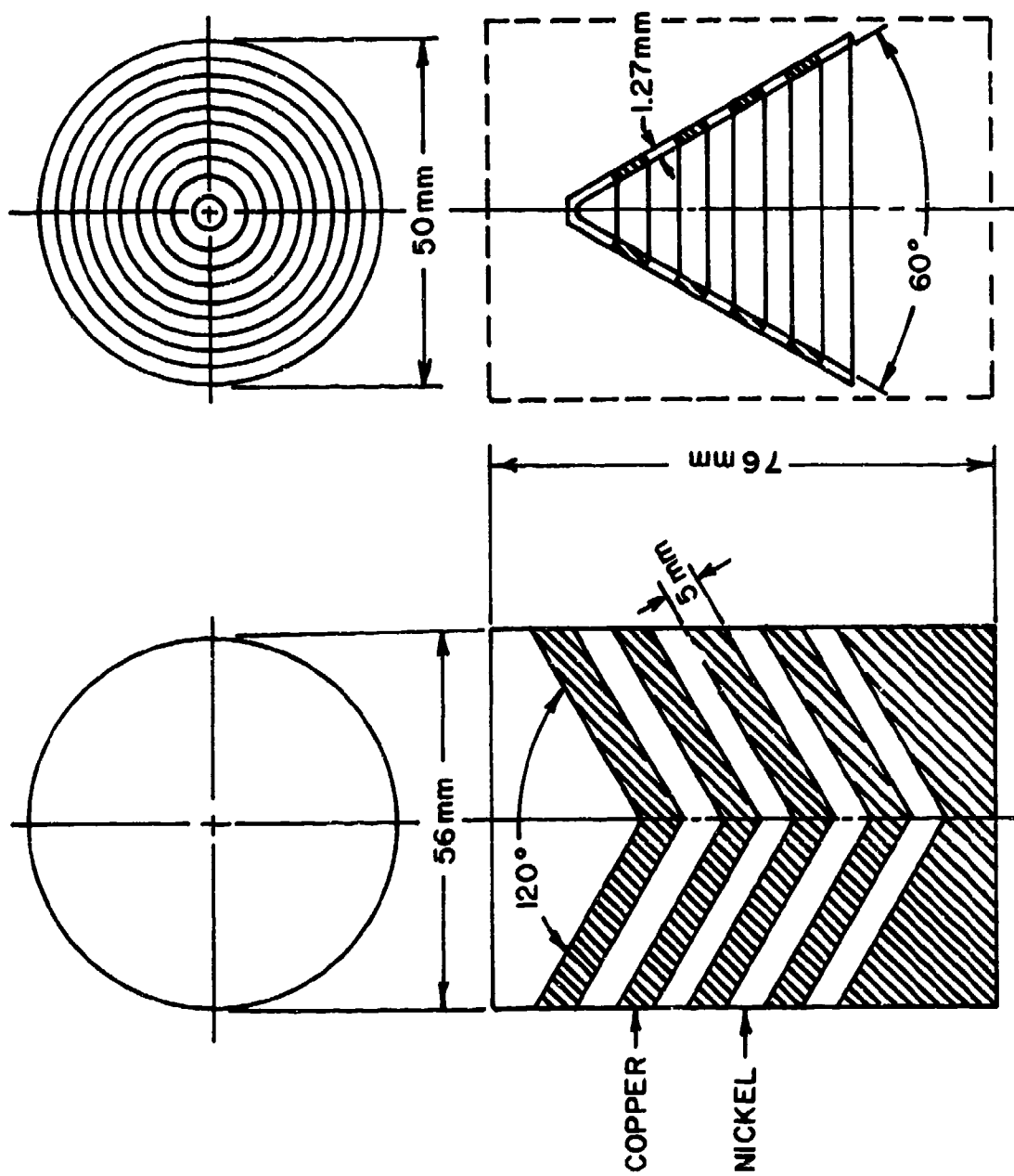


Figure 21. Diffusion bonding setup for fabricating stratified copper-nickel conical shaped-charge liners.

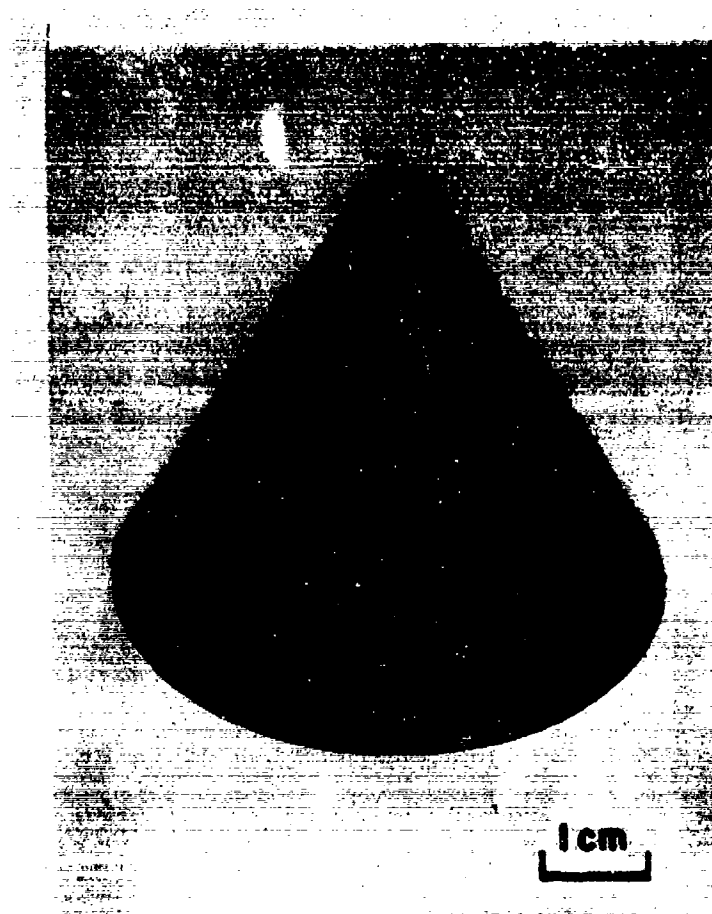
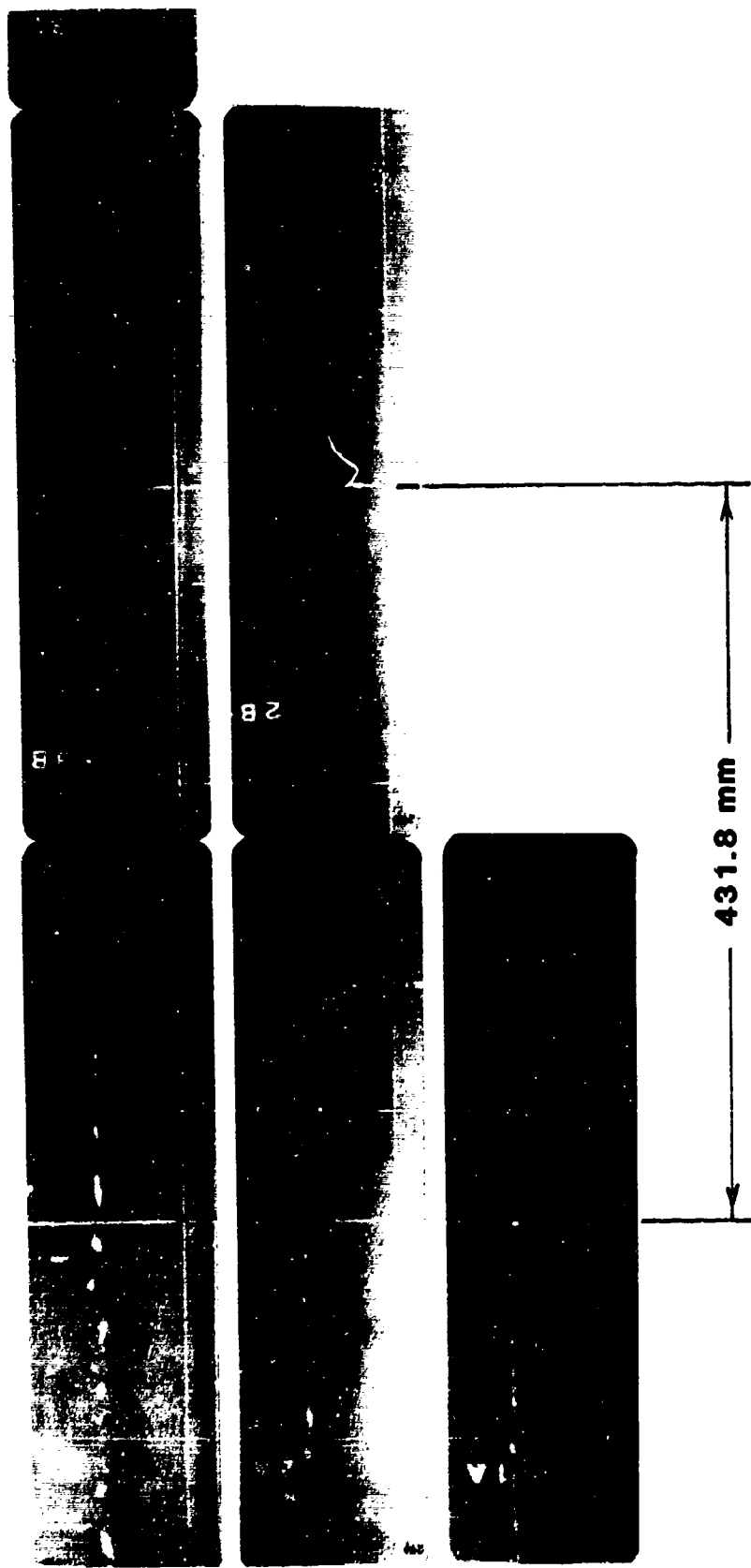


Figure 22. Finish machined, stratified, copper-nickel, conical shaped-charge liner.



times 81.3, 126.2 and 171.0 μ sec.

Figure 23. Free-flight flash radiographs of the jet from a stratified copper-nickel conical shaped-charge liner.

The largest of the recovered jet particles are shown in Figure 24. Note that both metals are present. The cross section of this particle is presented in Figure 25. The tubular construction is clearly shown. The central region of Figure 25 was enlarged and is shown in Figure 26. Finally, the recovered slug and a cross section of the slug is shown in Figure 27.

The flow patterns observed for the stratified, bimetallic, conical liner may or may not agree with the analytical results reported earlier, depending on the position of the recovered particles in the jet. At any rate, the recovered slug and conical liner jet particles reveal a flow pattern that has not been observed before. Eight of the nine original material layers are apparent.

6. SUMMARY AND CONCLUSIONS

The "tubular-layered" liner collapse and jet formation theory for point-initiated hemispherical liners has been verified, at least in part. (Complete verification of the collapse and formation is not possible since only a few jet particles were recovered). Also, flow patterns for a stratified, bimetallic, conical liner were obtained for the slug and a few jet particles. For both liner geometries, the experiments tended to support the a priori theoretical calculations. (See the CWCW report).

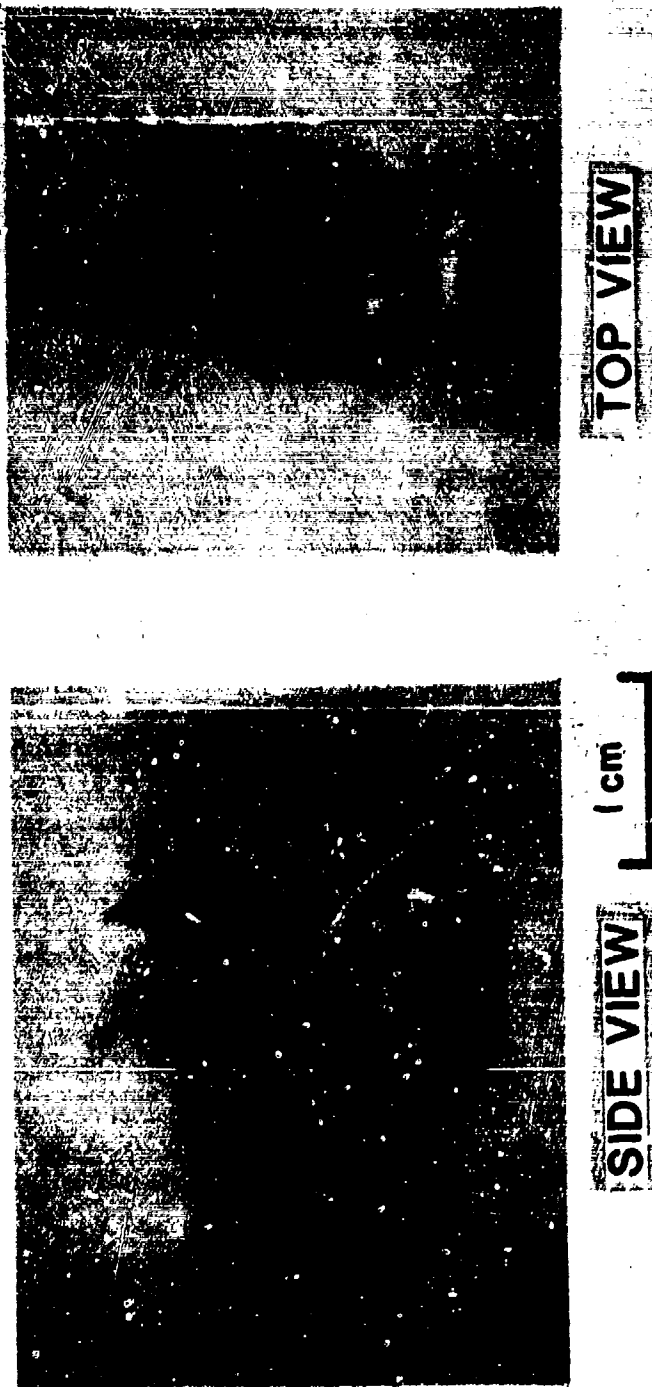
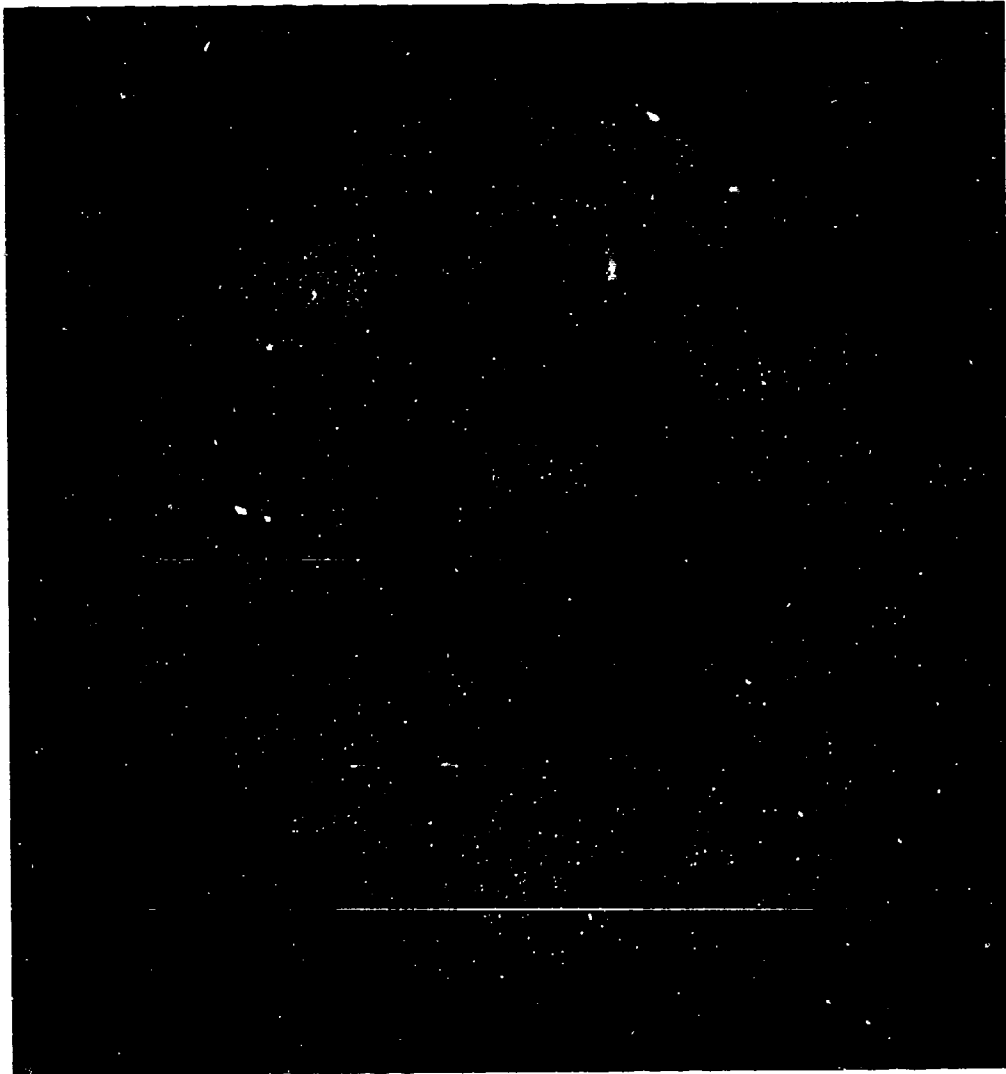
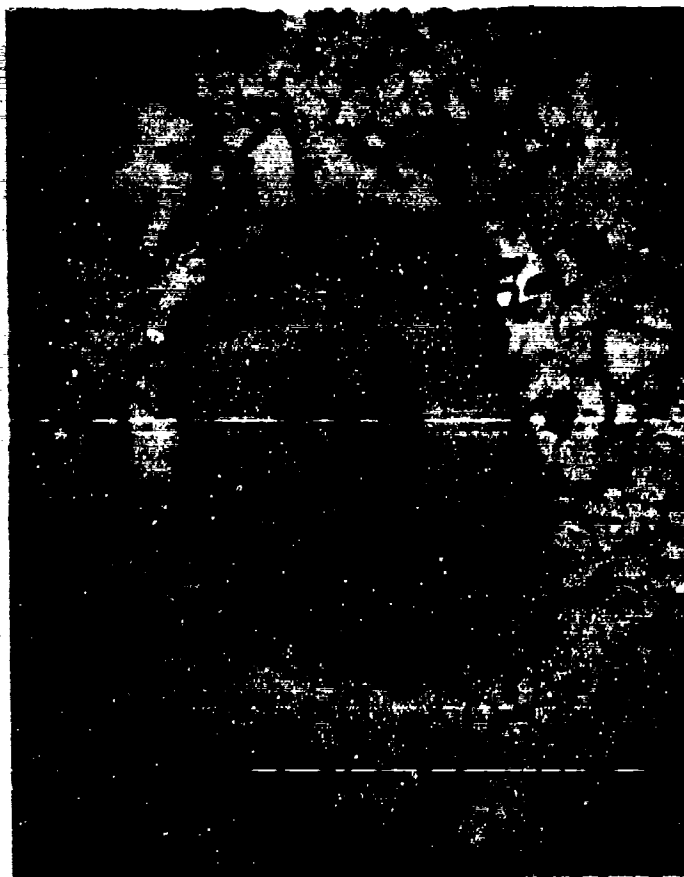


Figure 24. Jet particle from a stratified copper-nickel conical shaped-charge liner.



50 X

Figure 25. Cross section of jet particle from a stratified copper-nickel shaped-charge liner.



200X

Figure 26. Central region of jet particle from a stratified copper-nickel conical shaped-charge liner.

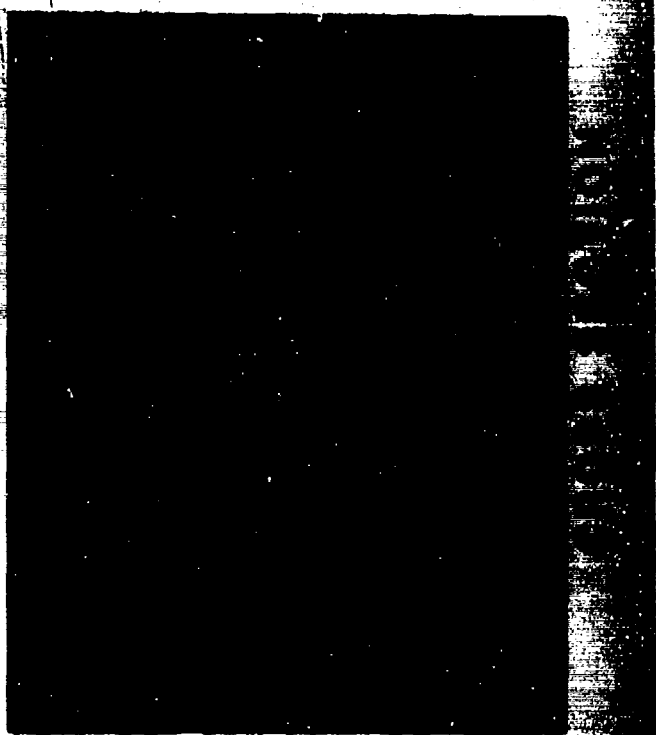


Figure 27. Recovered slug from a stratified copper-nickel conical shaped-charge liner.

LIST OF REFERENCES

1. Chou, P. C., Walters, W. P., Ciccarelli, R. D., and Weaver, G. W., "Jet Formation Mechanics of Hemispherical Warheads," BRL Contractor Report, BRL-CR-545, October, 1985.
2. Perez, E., Fauguignon, C. and Chanteret, P., "Fundamental Studies of Shaped Charge Mechanisms", Proceedings on the Third International Symposium on Ballistics, Karlsruhe, Germany, March 1977.
3. Brandes, E. A., editor, Smithells Metals Reference Book, Sixth Edition, Diffusion Bonding, pgs. 33-10 to 33-13, Butterworths, 1983.
4. Metals Handbook, 9th Edition, Vol. 6, Welding, Brazing, Soldering, pgs. 672-691, American Society for Metals, Metals Park, OH, 1983.
5. Barnes, R. S. and Mazey, D. J., "The Effect of Pressure Upon Void Formation in Diffusion Couples", Acta Metallurgica, Vol. 6, Jan. 1958.

DISTRIBUTION LIST

<u>Copies</u>	<u>Organization</u>	<u>Copies</u>	<u>Organization</u>
3	Commander MICOM Research, Development and Engineering Center ATTN: Library Joel Williamson M. C. Schexnayder Redstone Arsenal, AL 35898	10	Commander Naval Surface Weapons Center ATTN: Code DG-50 DX-21, Lib Br N. Coleburn, R-13 T. Spivok W. Reed, R10A R. Phinney C. Smith E. Johnson W. Bullock C. Dickerson White Oak, MD 20910
1	Assistant Secretary of the Army (R&D) ATTN: Assistant for Research Washington, DC 20310	1	Commander Naval Surface Weapons Center ATTN: Code 730, Lib Silver Spring, MD 20910
2	Commander US Army Material Technology Laboratory ATTN: AMXMR-RD, J. Mescall Tech Lib Watertown, MA 02172	1	Commander Naval Surface Weapons Center ATTN: DX-21, Lib Br Dr. W. Soper Dahlgren, VA 22448
1	Commander US Army Research Office P.O. Box 12211 Research Triangle Park NC 27709-2211	2	Commander Naval Weapons Center ATTN: Code 4057 Code 45, Tech Lib China Lake, CA 93555
1	Commander US Army Foreign Science and Technology Center ATTN: AIAST-IS 220 Seventh Street, NE Charlottesville, VA 22901-5396	2	David W. Taylor, Naval Ship R&D Center ATTN: D. R. Garrison/ Code 1740.3 H. Gray Bethesda, MD 20084
1	Commander Det S, USAOG USAINSCOM ATTN: IAGPC-S Ft. Meade, MD 20755	1	Commander Naval Research Laboratory Washington, DC 20375
2	Commander Naval Air Systems Command ATTN: Code AIR-310 Code AIR-350 Washington, DC 20360	1	USAF/AFRDDA Washington, DC 20330
1	Office of Naval Research Department of the Navy 800 N. Quincy Street Arlington, VA 22217	1	AFSC/SDW Andrews AFB Washington, DC 20311
		1	US Air Force Academy ATTN: Code FJS-41 (NC) Tech Lib Colorado Springs, CO 80840

DISTRIBUTION LIST

<u>Copies</u>	<u>Organization</u>	<u>Copies</u>	<u>Organization</u>
1	AFATL/DLJR (J. Foster) Eglin AFB, FL 32542	6	Sandia Laboratories ATTN: Dr. W. Herrman Dr. J. Asay Dr. R. Longcope Dr. R. Sandoval Dr. M. Forrestal Dr. J. Stephens Albuquerque, NM 87115
9	Director Lawrence Livermore Laboratory ATTN: Dr. J. Kury Dr. M. Wilkins Dr. E. Lee Dr. H. Horning Dr. M. Van Thiel Dr. C. Cline Dr. T. Ennis Dr. R. Wienguard Technical Library P.O. Box 808 Livermore, CA 94550	1	Systems, Science & Software ATTN: Dr. R. Sedgwick P.O. Box 1620 La Jolla, CA 92037
1	Battelle-Columbus Laboratories ATTN: Technical Library 505 King Avenue Columbus, OH 43201	2	General Dynamics Pomona Division ATTN: E. LaRocca, MZ4-40 R. Strike P.O. Box 2507 Pomona, CA 91769
2	Dyna East Corporation ATTN: P. C. Chou R. Cicccarelli 3432 Market Street Philadelphia, PA 19104-2588	5	University of California Los Alamos Scientific Lab ATTN: Dr. J. W. Hall Dr. R. K. Dr. L. Hull Mr. J. Repa Technical Library P.O. Box 1663 Los Alamos, NM 87545
1	Aerojet Ordnance Corporation ATTN: Warhead Tech. Dept. Dr. J. Carleone 2521 Michelle Drive Tustin, CA 92680	1	University of Denver Research Institute ATTN: Mr. R. F. Recht P. O. Box 10127 Denver, CO 80208
1	Physics International Company Tactical Systems Group Eastern Division ATTN: R. Berus P. O. Box 1004 Wadsworth, OH 44281-0904	2	University of Illinois Dept of Aeronautical and Astronautical Engineering ATTN: Prof. A. R. Zak Prof. S. M. Yen Campus Police Building 101 N. Matthews Urbana, IL 61801
2	Honeywell, Inc. Government and Aeronautical Products Division ATTN: G. Johnson J. Houlton 600 Second Street, NE Hopkins, NM 55343		

DISTRIBUTION LIST

<u>Copies</u>	<u>Organization</u>	<u>Copies</u>	<u>Organization</u>
2	California Research and Technology ATTN: Dr. Ronald E. Brown Mr. Mark Majerus 11875 Dublin Blvd. Suite B-130 Dublin, CA 94568	2	Boeing Aerospace Co. Shock Physics & Applied Math Engineering Technology ATTN: R. Helzer J. Shrader P. O. Box 3999 Seattle, WA 98124
1	University of Dayton Research Institute ATTN: Dr. S. J. Bless Dayton, OH 45469	1	McDonnell Douglas Astronautics Company ATTN: Bruce L. Cooper 5301 Bolsa Avenue Huntington Beach, CA 92647
2	Southwest Research Institute ATTN: C. Anderson A. Wenzel 6220 Culebra Road P. O. Drawer 28510 San Antonio, TX 78284	1	Commander Air Force Wright Aeronautical Laboratory A. F. Systems Command ATTN: Dr. Lee Kennard, ASD/PMRRC USAF Wright Patterson AFB Ohio 45443
2	Nuclear Metals Inc. ATTN: M. Walz W. Zimmer 2229 Main Street Concord, MA 01742	1	D. R. Kennedy and Associates Inc. ATTN: Donald Kennedy P. O. Box 4003 Mountain View, CA 94040
2	SRI International ATTN: Dr. L. Seaman Dr. C. Schmidt 333 Ravenswood Avenue Menlo Park, CA 94025		
1	Northrop Corporation Electro-Mechanical Division ATTN: Donald L. Hall 500 East Orangethorpe Avenue Anaheim, CA 92801		

Aberdeen Proving Ground

Dir, USAMSAA
ATTN: AMXSY-GI, B. Simmons

DISTRIBUTION LIST

<u>No. of Copies</u>	<u>Organization</u>	<u>No. of Copies</u>	<u>Organization</u>
12	Administrator Defense Technical Info Center ATTN: DTIC-DDA Cameron Station Alexandria, VA 22304-6145	1	Director US Army Air Mobility Research and Development Laboratory Ames Research Center Moffett Field, CA 94035
1	HQDA (DAMA-ART-M) Washington, DC 20310	1	Commander US Army Communications- Electronics Command ATTN: AMSEL-ED Fort Monmouth, NJ 07703
1	Commander US Army Materiel Command ATTN: AMCDRA-ST 5001 Eisenhower Avenue Alexandria, VA 22333-0001	1	Commander ERADCOM Technical Library ATTN: DELSD-L (Reports Section) Fort Monmouth, NJ 07703-5301
1	Commander Armament R&D Center US Army AMCCOM ATTN: SMCAR-TSS Dover, NJ 07801	1	Commander US Army Missile Command Research, Development and Engineering Center ATTN: AMSMI-RD Redstone Arsenal, AL 35898
1	Commander Armament R&D Center US Army AMCCOM ATTN: SMCAR-TDC Dover, NJ 07801	1	Director US Army Missile & Space Intelligence Center ATTN: AIAMS-YDL Redstone Arsenal AL 35898-5500
1	Director Benet Weapons Laboratory Armament R&D Center US Army AMCCOM ATTN: SMCAR-LCB-TL Watervliet, NY 12189	1	Commander US Army Tank-Automotive Cmd ATTN: AMSTA-TSL Warren, MI 48397-5000
1	Commander US Army Armament, Munitions and Chemical Command ATTN: SMCAR-ESP-L Rock Island, IL 61299	1	Director US Army TRADOC Systems Analysis Activity ATTN: ATAA-SL White Sands Missile Range NM 88002
1	Commander US Army Aviation Research and Development Command ATTN: AMSAV-E 4300 Goodfellow Blvd St. Louis, MO 63120	1	Commandant US Army Infantry School ATTN: ATSH-CD-CSO-OR Fort Benning, GA 31905

DISTRIBUTION LIST

<u>No. of Copies</u>	<u>Organization</u>	<u>ABERDEEN PROVING GROUND</u>
1	Commander US Army Development and Employment Agency ATTN: MODE-TED-SAB Fort Lewis, WA 98433	Dir, USAMSAA ATTN: AMXSY-D AMXSY-MP (H. Cohen)
1	AFWL/SUL Kirtland AFB, NM 87117	Cdr, USATECOM ATTN: AMSTE-TO-F
1	AFATL/DLODL Eglin AFB, FL 32542-5000	Cdr, CRDC, AMCCOM ATTN: SMCCR-RSP-A SMCCR-MU SMCCR-SPS-IL
10	Central Intelligence Agency Office of Central Reference Dissemination Branch Room GE-47 HQS Washington, DC 20502	

★ U.S. GOVERNMENT PRINTING OFFICE: 1987-491-890/40007

UNCLASSIFIED

USER EVALUATION SHEET/CHANGE OF ADDRESS

This Laboratory undertakes a continuing effort to improve the quality of the reports it publishes. Your comments/answers to the items/questions below will aid us in our efforts.

1. BRL Report Number _____ Date of Report _____

2. Date Report Received _____

3. Does this report satisfy a need? (Comment on purpose, related project, or other area of interest for which the report will be used.) _____

4. How specifically, is the report being used? (Information source, design data, procedure, source of ideas, etc.) _____

5. Has the information in this report led to any quantitative savings as far as man-hours or dollars saved, operating costs avoided or efficiencies achieved, etc? If so, please elaborate. _____

6. General Comments. What do you think should be changed to improve future reports? (Indicate changes to organization, technical content, format, etc.) _____

CURRENT
ADDRESS

Name _____
Organization _____
Address _____
City, State, Zip _____

7. If indicating a Change of Address or Address Correction, please provide the New or Correct Address in Block 6 above and the Old or Incorrect address below.

OLD
ADDRESS

Name _____
Organization _____
Address _____
City, State, Zip _____

(Remove this sheet along the perforation, fold as indicated, staple or tape closed, and mail.)

UNCLASSIFIED

UNCLASSIFIED

----- FOLD HERE -----

Director
U.S. Army Ballistic Research Laboratory
ATTN: SLCBR-DD-T
Aberdeen Proving Ground, MD 21005-5066

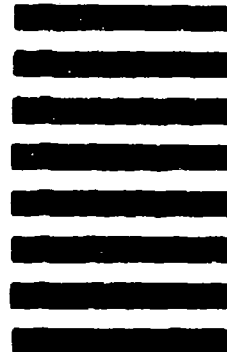


NO POSTAGE
NECESSARY
IF MAILED
IN THE
UNITED STATES

OFFICIAL BUSINESS
PENALTY FOR PRIVATE USE, \$300

BUSINESS REPLY MAIL
FIRST CLASS PERMIT NO 12062 WASHINGTON, DC
POSTAGE WILL BE PAID BY DEPARTMENT OF THE ARMY

Director
U.S. Army Ballistic Research Laboratory
ATTN: SLCBR-DD-T
Aberdeen Proving Ground, MD 21005-9989



----- FOLD HERE -----

UNCLASSIFIED